12-13-2003

Dehydration of an Ethanol/Water Mixture Using Lignocellulosic Based Adsorbents

Tracy John Benson

DEHYDRATION OF AN ETHANOL/WATER MIXTURE USING LIGNOCELLULOSIC BASED ADSORBENTS

By

Tracy John Benson

A Thesis
Submitted to the Faculty of
Mississippi State University
in Partial Fulfillment of the Requirements
for the Degree of Master of Science
in Chemical Engineering
in the Dave C. Swalm School of Chemical Engineering

Mississippi State, Mississippi

December 2003

DEHYDRATION OF AN ETHANOL/WATER MIXTURE USING

LIGNOCELLULOSIC BASED ADSORBENTS

By

Tracy John Benson

Approved:

Clifford E. George Professor of Chemical Engineering (Major Professor)	Mark E.Zappi Professor of Chemical Engineering (Committee Member)
Hossein Toghiani Associate Professor of Chemical Engineering (Committee Member)	Tor P. Schultz Professor of Forest Products (Committee Member)
Mark E. Zappi Professor of Chemical Engineering (Graduate Coordinator of Dave C. Swalm School of Chemical Engineering)	A. Wayne Bennett (Dean of the College of Engineering)

Name: Tracy John Benson

Date of Degree: December 13, 2003

Institution: Mississippi State University

Major Field: Chemical Engineering

Major Professor: Dr. Clifford E. George

Title of Study: DEHYDRATION OF AN ETHANOL/WATER MIXTURE USING LIGNOCELLULOSIC BASED ADSORBENTS

Pages in Study: 120

Candidate for Degree of Master of Science

This study evaluated the effectiveness of using cellulosic adsorbents to dehydrate 95 wt% ethanol/5 wt% water mixture. Hardwood sawdust, kenaf core, and bleached wood pulp were used as adsorbents in both liquid phase and gas phase experiments.

All three adsorbents preferentially adsorbed water compared to ethanol. Bleached wood pulp exhibited the best performance of adsorbents examined. Data from the liquid – phase experiments were fitted to the Chakravarti – Dhar isotherm equation. From the vapor – phase experiments, the average water loading of hardwood sawdust, kenaf core, and bleached wood pulp was 0.0037, 0.0076, and 0.0121 g H_2O/g adsorbent, respectively. Two methods, the Colburn J Factor and the Thoenes – Kramers correlation, were used to evaluate the mass transfer coefficient of water. Furthermore, the surface area of the adsorbents was measured using the B.E.T. method. Surface areas were 4.91, 9.99, and 8.84 m^2/g for the hardwood sawdust, kenaf core, and the bleached wood pulp, respectively.

DEDICATION

I would like to dedicate this research to my parents, Carl and Nancy Benson, whose never-ending support has been the motivation for this work.

ACKNOWLEDGEMENTS

I want to express my gratitude to my major professor, Dr. Clifford E. George, for providing me the chance to pursue my Master's degree in Chemical Engineering and for being so patient with me in the past three years. Dr. George has been a great help and inspiration to me. He is readily available to answer my questions and to give direction to my research. Also, I want to say thank you to my committee members, Dr. Tor Schultz, Dr. Hossein Toghiani, and Dr. Mark Zappi. They have been as helpful as Dr. George. I would especially like to thank Dr. Zappi for his help and direction with laboratory equipment. I am also thankful to the United States Department of Energy for the financial support of my project.

I am also extending my gratitude to the undergraduate students who have worked on this project with me: Britton Eyles, Maxine Jones, Katrina Parker, and Tara Smith. My deep appreciation goes to all of my fellow colleagues, especially the members of the ETECH lab. I would also like to thank Mrs. Sherre Denson and Ms. Ellen Weeks for their help with office needs and assistance. Thanks are also due to Mr. Wayne Phelps for his assistance with the experimental setup.

TABLE OF CONTENTS

APPENDIX

LIST OF TABLES

TABLE Page

LIST OF FIGURES

FIGURE Page

FIGURE Page

CHAPTER I

INTRODUCTION

Background

It is predicted that by the year 2020 energy needs will have increased to the point that 18 million barrels of crude oil per day will be needed to operate regular automobiles, light trucks, and heavy trucks in the United States. Consumption for the year 2000 was 12 million barrels per day (DOE, 2001). To meet the growing demand, new sources of energy, especially renewable resources, must be developed. The production of ethanol from biomass is one such potential source. Biomass is defined as any naturally growing, plant-derived substance including, but not limited to, trees, switch grasses, agricultural food crops, and crop wastes (DOE, 2001). The polysaccharides in biomass can be processed into ethanol and used as a motor fuel additive or directly as fuel. The addition of ethanol to gasoline eliminates the need for MTBE as an octane enhancer. The use of ethanol in automobiles will displace a significant amount of gasoline, thereby reducing the amount of crude oil needed for transportation.

During the production of ethanol, large quantities of water are discharged from the fermenter along with the ethanol. The fermenter effluent typically has an ethanol

concentration of approximately 10 percent, by weight. This ethanol/water mixture must be separated to produce ethanol with a purity sufficient to be blended with gasoline.

Dehydration of ethanol has been a widely studied topic that has taken many centuries to develop. At first, it was only necessary to concentrate ethanol from a fermentation broth for the purpose of producing alcoholic beverages and for producing alcohol for use as a sterilization agent. Alcohol for these purposes was refined through distilling processes and only required ethanol concentrations of up to about 85 wt%. Since the mid-1970's, it has been proposed that ethanol be used an octane enhancer to gasoline. This requires an ethanol concentration of 99.5 wt% or higher.

Purification Beyond the Azeotrope

The high purity of ethanol needed for automobile use has created a new dilemma. Distillation can only be used to remove water from aqueous ethanol to achieve a maximum ethanol concentration of 95.6 wt%. At this concentration, the ethanol and the water boil at the same temperature. This constant boiling mixture is called an azeotrope. Since distillation can only be used to separate mixtures that have different boiling temperatures, new methods of separation must be employed to accomplish further dehydration.

There are several methods of product separation that will purify ethanol past the azeotropic level. These methods include vacuum distillation, azeotropic distillation, and extractive distillation. However, for the large quantities of ethanol that are needed for the automotive industry, these processes are largely uneconomical. Therefore, it has been proposed that aqueous ethanol dehydration be accomplished through the use of

adsorption. An industrial column can be packed with an adsorbent that will preferentially adsorb water, leaving pure ethanol as the effluent product. Using this method of separation requires identification of adsorbents that will readily adsorb water during the adsorption phase of operation but also will easily desorb the water during the regeneration phase.

Adsorbents that readily adsorb water have already been examined and are in commercial use (Davis and Kristen, 1974; Grethlein and Thomas, 1992). Molecular sieves were the first adsorbent to be used. The biggest drawback with molecular sieves is the high cost of regeneration because of the high temperatures required to desorb the water that collects within the pores.

This has driven the search for new and more efficient adsorbents. Dr. Michael Ladisch at Purdue University began to investigate the use of natural materials as adsorbents (Ladisch, 1979). In the early 1980's, he proposed and patented the use of corn grits as a water adsorbent. With this discovery, a new approach to the ethanol dehydration problem emerged. It was found that biomass materials were generally less expensive to regenerate when compared to the molecular sieves (Ladisch, 1982). Also, if regeneration was not feasible, the biomass adsorbent could be used as a feedstock to the fermenter at the forefront of the chemical process.

Biomass materials that have been investigated and found to be viable adsorbents include corn grits, potato starch, amylose, and maize starch. These materials are starch-based adsorbents with high levels of amylopectin. Another class of adsorbents, such as wheat straw and woodchips, are derived from cellulosic-based materials. These materials use xylans and cellulose as the major adsorbing mechanism instead of amylopectin.

Little research, however, has been performed on cellulosic materials. It is currently unclear which materials will provide the highest degree of adsorption at the lowest cost.

The cost factor is assessed, not only in terms of water uptake efficiency, but also on regeneration or adsorbent replacement costs. If the material is to be replaced after each adsorption run, then the adsorbent must be cheaply, readily available, and easily and safely disposed. Starch adsorbents based from corn are readily available in the Midwestern United States where corn is a common crop. In the Southern United States region, however, corn is not as readily available as are cellulosic materials. Therefore, for an ethanol producer in the Southeastern United States, it would be cost prohibitive to transport starch materials across long distances when a more suitable adsorbent could be obtained locally.

Statement of the Problem and Research Objective

Cellulosic biomass adsorbents can be used to remove the residual water that is left after distillation of ethanol fermenter effluents. The effective capacity and economical viability of these adsorbents remain largely unknown to scientists and engineers.

The specific objectives of this study were the following:

(1) Investigate to determine which lignocellulosic materials will readily adsorb water based upon the molecular makeup of the adsorbent and to determine the feasibility of using lignocellulosic adsorbents instead of starch-based adsorbents.

(2) Identify the underlying mechanisms of the adsorption phenomenon to increase adsorption capacity and adsorption rate.

(3) Calculate the values of the mass transport characteristics such as Schmidt's Number and mass transport diffusivity.

(4) Evaluate the macro-dynamic column effects such as length and velocity of the Mass Transfer Zone.

This research project is a preliminary study that develops the characteristics of water adsorption onto cellulosic materials for the purification of ethanol. The adsorption experiments should be applied on a pilot scale basis to have a better understanding of how the exothermic nature of adsorption will affect an industrial adsorber.

CHAPTER II

LITERATURE REVIEW

A review of the literature on the separation of ethanol and water during the production of ethanol by fermentation has shown that the process can be divided into two stages. The first stage is to distill the fermentation products, which is beer, from about 8 wt % ethanol to just below the azeotropic composition (95.6 wt % ethanol). The mixture is often distilled to achieve a distillate of approximately 85 wt % ethanol. Further concentration of ethanol/water mixture of 85 wt % to the azeotrope requires several column stages and high reflux ratios which necessitates the use of high amounts of energy for a small degree of separation (Ladisch, 1979). The second stage involves a dehydration step to remove the remaining water from the ethanol. Dehydration technologies can be classified into four types:

(i) Low Pressure Distillation

(ii) Azeotropic Distillation

(iii) Extractive Distillation

(iv) Adsorption

Low Pressure Distillation

The azeotrope that exists between ethanol and water is pressure dependent and vanishes as the pressure inside a distillation column is lowered to 11.5 kPa. Therefore, it is possible to completely separate the mixture and obtain ethanol as a distillate. According to Black's (1980) modeling efforts, he found this separation approach to be uneconomical. In his modeling work, the energy consumed by the dehydration process was greater than the thermal energy of combustion (23,412.3 kJ/L) for the resulting product. A column requiring 60 trays and a reflux ratio of 9.7 is necessary to achieve the necessary separation.

Azeotropic Distillation

With azeotropic distillation, a solvent, or entrainer, is added to the ethanol/water mixture which will form an azeotrope with either the ethanol or the water, or perhaps both. The entrainer increases the relative volatility of one of the components over the other allowing for complete separation (Black, 1980). Azeotropic distillation is an especially suitable method of separation if the newly formed azeotrope is heterogeneous. A heterogeneous azeotrope is one in which condensing vapors form two separate, immiscible liquid phases (Wankat, 1988). Azeotropic distillation requires an additional unit operation that will separate the extra-added solvent so that it can be recycled. The distillate is condensed forming a solvent rich phase and a heavier aqueous phase.

For the dehydration of aqueous ethanol, selection of the right entrainer is extremely important. The solvent selected must form an azeotrope that boils at a low

enough temperature to be removed as a distillate and also is easily removed in a stripping column. Moreover, the entrainer must be nontoxic, noncorrosive, chemically stable, readily available, and relatively inexpensive (Wankat, 1988). Even though benzene and diethyl ether have been commercially used, n-pentane is a more efficient entrainer. According to Black, the use of n-pentane as an entrainer results in a dehydrated ethanol with the lowest water content compared to benzene or diethyl ether as entrainers. Also, the column reboiler heat duty for n-pentane is approximately 60% less than that for benzene and 80% less than that for diethyl ether. Furthermore, n-pentane requires fewer column trays and a smaller column diameter than benzene or diethyl ether, resulting in lower capital costs (Black, et al., 1972).

Azeotropic distillation using n-pentane as the entrainer allows for complete recovery of dehydrated ethanol. The dehydrated ethanol leaves the azeotropic column as the bottoms product. The overhead stream is condensed, forming a heterogeneous azeotrope. The upper layer, which is rich in n-pentane, is refluxed back to the azeotropic column. The bottom, aqueous layer is fed to a stripping column to remove the water. The remaining ethanol and n-pentane are added to the upper layer and used as reflux (Black, 1980).

The energy requirements for azeotropic distillation are much lower than for low pressure distillation; however, the energy required for ethanol dehydration exceed the combustible energy of ethanol. The reboiler duty for azeotropic distillation has been calculated to be about 2,066 kJ/L, and the condenser duty has been calculated to be about –2077 kJ/L. Also, the column is operated at 331.5 kPa versus 10.2 kPa in a low pressure

column resulting in lower operating costs. The reboiler and condenser duties for the stripping column are 550 kJ/L and –468 kJ/L, respectively (Black, 1980).

Extractive Distillation

Extractive distillation is similar to azeotropic distillation in that a solvent is added to the dehydration column; but, unlike azeotropic distillation, the chosen solvent does not form an azeotrope with any of the components being separated. In either case, a solvent is added to alter the nonideal behavior of the ethanol/water system by altering the molecular environment. In extractive distillation, the solvent is added to the dehydration column above the feed stream and is found to be in high concentrations in the liquid phase in the stripping section of the column. Thus, the solvent is removed as a mixture in the bottoms product (Black and Ditsler, 1972). The chosen solvent usually has a significantly higher boiling point than either of the two components being separated and is selectively attracted to one of the components, reducing the volatility of that component. The other component in the mixture now exhibits a higher relative volatility and is easily removed as the distillate product. It is typical to operate an extractive distillation column with a solvent flow rate feed that is 1, 5, 10, 20, or even 30 times that of the feed flow rate (Wankat, 1988).

A solvent's selectivity, or more precisely, the solvent's ability to affect the behavior of the other components in a solution to an extent that the relative volatilities are changed, are due to molecular interactions. Both physical and chemical forces contribute to a solvent's selectivity. The physical forces are classified as dispersion forces, induction forces, and orientation forces and are thermodynamically endothermic. The

chemical forces at work are hydrogen bonding and complexing of the molecules in solution and are found to be thermodynamically exothermic (van Winkle, 1967). Another factor in a solvent's selectivity is its polarity. A solvent can be chosen such that it will adhere to either the least polar or more polar of the two components being separated. Hydrogen bonding, however, appears to be more important in determining a solvent's selectivity than polarity; thus, it is advisable to select a solvent based upon its hydrogen bonding characteristics rather than its polarity (Wankat, 1988).

If anhydrous ethanol is to be used as a gasoline fuel additive, then gasoline itself is for a good solvent. According to Black (1972), the gasoline is more non-ideal with water than with ethanol, thus causing the water to boil at a lower temperature than the ethanol/gasoline mixture, and the water is removed as a distillate. The bottoms product is a mixture of ethanol, gasoline, and trace amounts of water. A stripping column is necessary to remove any remaining ethanol and gasoline from the overhead product. The ethanol and gasoline that are removed are then added to the ethanol/gasoline product. At this point, additional gasoline can be added to produce the proper concentration for gasohol. The drawback of using gasoline is that its high volatility makes it a safety risk and care must be taken to prevent explosion of the vapors.

The energy requirements for extractive distillation using gasoline as the added solvent are significantly lower than for azeotropic distillation. The reboiler duty for extractive distillation is approximately 1,577 kJ/L, and the condenser duty has been calculated to be about –1,393 kJ/L. The reboiler and condenser duties for the stripping column are 520 kJ/L and –443 kJ/L, respectively (Black, 1980).

While gasoline has been shown to be an economical additive for extractive distillation, other solvents are not. One such solvent is ethylene glycol. Based upon modeling results published by Black and coworkers (1972), azeotropic distillation using n-pentane as the entrainer is more economical than extractive distillation using ethylene glycol. They reported that an extractive distillation process has a reboiler duty of 3445.6 kJ/L and a condenser duty of –2,162.8 kJ/L for the extraction column, and reboiler and condenser duties for the stripping column are 1,538.0 kJ/L and –1,319.4 kJ/L, respectively.

Table 2.1 summarizes the comparison of low-pressure, azeotropic, and extractive distillations for the dehydration of ethanol based upon an ethanol feed rate of 32.5 kg mol/hr and an ethanol concentration of 83 mole-percent. For azeotropic and extractive distillations, the values shown in Table 2.1 for the condenser duty and reboiler duty include the energy requirements for both the distillation column and the stripping column to remove the "added" component.

Table 2.1. Comparison of Traditional Ethanol/Water Dehydration Practices

Dehydration Technique	Condenser Duty (KJ/L)	Reboiler Duty (KJ/L)	Percent of Ethanol Heating Value
Low-pressure Distillation	-4,298.0	4,137.8	43.3
Azeotropic Distillation (solvent – pentane)	-2,540.1	2,616.2	36.8
Extractive Distillation (solvent – gasoline)	-1,836.9	2,098.3	34.6

Adsorption

Adsorptive distillation can be defined as any adsorption process that uses an active column packing for the purpose of separating or purifying chemical mixtures. Currently, adsorption using molecular sieves is the leading method of breaking the ethanol/water azeotrope. Adsorption does not require additional unit operations to separate added solvents and/or entrainers (Abu, et al., 1999).

The active packing material can modify the intermolecular forces within a mixture to be separated, therefore, altering the vapor-liquid equilibrium of the mixture (Abu et al., 1999). It is imperative that the proper packing material is selected to efficiently and economically separate the mixture components. Surface area, chemical selectivity, and regeneration requirements are some of the factors govern the selection.

One of the largest concerns with selecting the proper adsorbent is surface area. Ethanol and water form a homogeneous mixture, but the presence of a solid adsorbent creates a heterogeneous system. The adsorption phenomena takes place at the interface between the ethanol/water gas phase and the solid adsorbent. It is commonly believed that the larger the surface area, the higher the adsorptive capacity of the adsorbent. Larger surface area can be achieved through the use of smaller sized packing. If the packing is too small, however, pressure drops sufficiently large enough to produce column flooding will occur. Larger surface area can also be generated from smaller pore sizes. It is important to find the optimum pore size. Smaller pores mean more surface area, but the pores have to be large enough to allow the adsorbed molecule to be adsorbed. In an ethanol/water mixture, an adsorbent with a nominal pore size of 3 to 4

Angstroms is necessary for water molecules to adsorb into the porous matrix. Molecular sieves have a typical surface area of 800 to 1,000 m^2/g (Schweitzer, 1996).

Chemical selectivity ensures that the active column packing adsorbs the proper component(s). For example, in the ethanol/water system, ethanol is the component that is marketable. Therefore, an adsorbent is needed that preferentially adsorbs water. Activated alumina, silica gel, and molecular sieves preferentially adsorb water over organic chemicals in a gas-phase adsorber (Schweitzer, 1996).

Another important factor in determining the proper adsorbent is its regeneration requirements. There is a maximum amount of adsorbed material that an adsorbent can hold. This maximum is the breakthrough or saturation amount. Once this threshold is reached, the adsorbent must be regenerated to remove the adsorbed material and prepare the adsorbent for reuse. Regeneration usually requires high temperatures and needs some type of gas (usually nitrogen, carbon dioxide, or air) to pass through the adsorbent bed to remove the contaminants (Schweitzer, 1996). This is true with the ethanol/water system. At Archer Daniels Midland (ADM), a commercial ethanol dehydration facility in Decatur, IL, there are several packed bed adsorbers that are in operation. These adsorption columns are packed with starch-based corn grits. Some are being used to dry the ethanol, while others are in the regeneration phase. A hot carrier gas is passed countercurrently through the column desorbing the water and preparing the adsorbent for another adsorption run. The hot carrier gas leaves the adsorbent bed, is cooled, and the water is condensed leaving the gas available for regeneration of another column (Grethlein and Nelson, 1992).

The two general types of adsorption packing for ethanol are (i) commercial synthetic materials, called zeolites, and (ii) naturally occurring materials called biomass.

(i) Commercial zeolites: Commercial zeolite adsorbent materials come in the form of activated alumina, silica gel, molecular sieves, and activated carbon. Of these, molecular sieves are commonly used for the dehydration of organic compounds. Molecular sieves are produced from metal aluminosilicates having a three-dimensional interconnecting crystalline structure of silica and alumina tetrahedral (Schweitzer, 1996). When using zeolite adsorbents, the ratio of silica to alumina can be adjusted to give a higher affinity for water (Ruthven, 1984). For the adsorption of water by silica, 1 mole of hydroxyl groups adsorbs 1 mole of water groups at a BET monolayer surface coverage (Gregg and Sing, 1982). Type A molecular sieves, the most commercially available, come in a variety of pellet sizes and pore sizes. UOP, a joint venture of Union Carbide and Allied Signal Inc., produces Molsiv® Adsorbent Type A molecular sieves ranging in pellet sizes from powder form up to 1/8-inch pellets with a bulk density of 40 lb/ft^3. UOP suggests using molecular sieves of a nominal pore size of 3 Angstroms for dehydration of unsaturated hydrocarbons and polar liquids such as ethanol (Davis and Manchanda, 1974). These molecular sieves have an average cross sectional area of 0.30 nm. Water molecules, with an approximate molecular diameter of 0.28 nm, can easily penetrate the pores of the molecular sieve adsorbent, while ethanol, with an approximate molecular diameter of 0.44 nm, cannot (Carmo and Gubulin, 1997).

Molecular sieve technology has been available for many years, but the high cost of regeneration has kept it from becoming a widely used dehydration process. Garg et al. (1983) have developed a new method of molecular sieve regeneration. Once

breakthrough has occurred and the adsorbent is saturated, instead of allowing the system to cool, the desorption step uses the stored heat energy that is produced from adsorption to aid in the regeneration cycle. This is a significant amount of heat with streams containing large amounts of water (up to 20 wt %); therefore, the volume and temperature of the regeneration purge is lessened thus making the desorption step more energy efficient (Garg and Ausikaitis, 1983).

Abu Al-rub and coworkers (1999) investigated the effectiveness of using molecular sieves for dehydration of ethanol. These experiments were conducted using an 800 ml recirculation still. Adding differing amounts of molecular sieves with 200 ml of ethanol/ water solution provided information on the adsorption mechanism.

Results indicate that the Vapor-Liquid Equilibrium of the ethanol/ water system had been altered due to reduction of non-idealities of the ethanol and water, and the azeotropic point had been removed in the presence of the molecular sieves with a feed of 95.6 wt% ethanol. Experiments were conducted using 3 and 4-Angstrom molecular sieves. The 3-Angstrom molecular sieves performed better, yielding greater separation of the mixture compared to the 4-Angstrom molecular sieves (Abu Al-Rub, et al., 1999). The reason may be credited to the fact that intermolecular interactions between the solid and liquid are inversely proportional to the pore diameter, and these long-range surface forces can be experienced over hundreds of nanometers leading to changes in physical properties of thin liquid layers on solids (Israelachvili, 1985).

Carmo and Gubulin (1997) investigated the kinetic and thermodynamic adsorption properties of the liquid-phase ethanol/water system on 3-Angstrom zeolites, both in spherical and cylindrical geometries. For the thermodynamic properties,

equilibrium adsorption isotherms were produced using a thermostated bath at temperatures of 25, 40, 50, and 60°C. Kinetic tests were performed using a liquid circulating device that allowed the ethanol/ water mixture to be recirculated through a bed of adsorbent. Thermodynamic results indicated that both geometries had the same adsorption capacities at all temperatures studied. The adsorptive capacity decreased with increasing temperature, and the Langmuir adsorption isotherm satisfactorily correlated the experimental data. The kinetic results denoted that an increase in temperature results in an increase in diffusivity of water for both cylindrical and spherical molecular sieve pellets (Carmo and Gubulin, 1997).

Crittenden and Sowerby (1990) explored vapor phase adsorption of water onto zeolite adsorbents. These experiments were carried out with 1.76 cm and 5.25 cm diameter adsorption columns. The columns were equipped with thermocouples axially along the column protruding into the column bed to study the effects of the heats of adsorption on column dynamics. Each column was packed to a height of 40 cm with 4-Angtrom molecular sieves. Variations in initial bed temperatures, feed flow rates, and feed concentrations were made to determine optimum operating conditions. The columns were heated to a desired operating temperature before each experimental run. The range of adsorption temperatures studied were 88 to 136°C for the small diameter column and 104 to 136°C for the large diameter column. The array of feed flow rates was between 0.24 and 0.67 cm^3 liquid/s, and variations in feed concentrations were between 4.86 and 12.26-wt% water (Crittenden and Sowerby, 1990).

From the data, the average loading of the molecular sieves with water and the Mass Transfer Zone (MTZ) could be evaluated. The MTZ is the zone in the adsorption

bed where a concentration gradient exists. The fixed-bed adsorption process is a dynamic one in which most of the adsorption of the contaminate takes place along the inlet of the column until the adsorbent of the inlet becomes saturated. Then the majority of adsorption moves to the next zone in the direction of fluid flow. This dynamic zone is the mass transfer zone and is a major factor in designing adsorption columns (Schweitzer, 1996).

The larger diameter column had earlier breakthrough of water, lower average bed loadings, longer MTZ's, and higher bed temperatures. Crittenden and Sowerby (1990) indicate that the selection of column diameter is a compromise between minimal capital costs and minimal operating costs. Also, the optimum operating conditions for the 5.25 cm column were a feed with a flow rate of 0.24 cm^3 liquid/ s, an initial bed temperature of 104°C, and a composition of 4.8 wt% water. These conditions resulted in an anhydrous ethanol product with a maximum bed loading of 0.106 g water/g adsorbent and a minimum MTZ length of 34.7 cm.

The differences in the desorption step between the two different sized columns were also considered. A nitrogen purge was used to remove the adsorbed water from the porous media. The flow rate of nitrogen, column pressure, and final column temperature were varied to determine the optimum criteria for the desorption step. The extent of desorption was increased by increasing the nitrogen flow rate, decreasing the column pressure, or by increasing the final bed temperature for the smaller column. For the larger diameter column, a reduced bed center temperature indicates a reduced rate of radial heat transfer. Consequently, the extent of desorption was considerably less (Crittenden and Sowerby, 1990).

(ii) Biomass Materials: Biomass adsorbents are a general term for all adsorbent materials that are naturally produced. These include, but are not limited to, starchy materials such as cornmeal, corn grits, cracked corn, starch, and cereal grains and lignocellulosic materials such as cellulose, wheat straw, bagasse, hemicellulose, and wood chips (Ladisch et al., 1984). When using starch-based biomass adsorbents, starch attracts the water molecule onto the adsorbent. For cellulosic adsorbents, the hemicelluloses and cellulose of the plant material are responsible for water adsorption. Hydrophilic polymers typically show sigmoidal shape isotherms and are classified as Type II Isotherms (Lee et al., 1991). Biomass materials offer an inexpensive and stable form of adsorbent. Ground corn requires less than 2,000 BTU/gal for regeneration as 190 proof ethanol is dehydrated (Bienkowski, 1986).

Ladisch (1984) examined the energy potential of dehydrating ethanol using starch materials and found that the dehydration step requires only one-tenth of the energy that is gained by combustion of ethanol. In contrast, the energy required for other dehydration methods exceeds that which is gained from ethanol combustion (Ladisch, et al, 1979). Based on the research of Ladisch, ADM has been using corn grits as a dehydrating adsorbent for ethanol since the 1980's (Grethlein and Nelson, 1992).

Crawshaw and Hills (1989) investigated the relative selectivities of various biomass adsorbents in the presence of ethanol and water. The adsorbents chosen had varying amounts of amylose and amylopectin, which are amorphous, alpha-linked glucan, commonly called starch. Maize starch and amica starch, both high in amylopectin, proved to be more selective in adsorbing water compared to ethanol. Also, adsorbent particle size was found to be an impact on the amount of ethanol adsorbed, but

not the amount of water adsorbed. It appears that ethanol adsorbs to a maximum depth of 60 μm, which was the average particle radius of the corn grits used in the experiment. By means of a "shrinking core" model, particles larger than 120 μm were identified as diffusion controlled (Crawshaw and Hills, 1989).

Amylose, shown in Figure 2.1, is a linear D-glucose polymer that comprises approximately 20% of starch. The glucose units are linearly linked by alpha 1-4 glycoside bonds with usually over 1,000 glucose units per amylose molecule. Amylose is only slightly soluble in water due to its large proportion of hydroxyl groups found in the inside of the molecule's helical structure and not in direct contact with water.

Amylopectin, on the other hand, is a branched D-glucose that comprises the other approximately 80% of starch. Amylopectin also contains α 1-4 units but has a degree of polymerization on the order of 10,000 to 100,000. Amylopectin, as shown in Figure 2.2, is often used in the food industry as a thickener in gravy due to its ability to adsorb water. The branched chain structure of amylopectin may be the factor accounting for its high ability to adsorb water. The branching causes an array of overlapping hydroxyl groups that strongly attract water molecules and trap them within the branched matrix (Rebar, et al., 1984).

Rebar et al. (1984) studied adsorption effects on four different starches: waxy-maize starch, cornstarch, potato starch, and potato amylose. Experiments were conducted with temperatures in the range of 50-90°C. Waxy-maize starch showed more water adsorption capabilities than the other three studied starches. Also, water proved to have much higher retention capability than ethanol (between 2,000 to 14,000 times more) in all

four starches and for all temperatures within the 50-90°C range. This preferential adsorption of water appeared to be correlated with its high amylopectin content. Furthermore, net retention times severely decreased with increasing temperature. For example, waxy-maize starch had a tenfold reduction (496.3 to 50.74 min) in net retention time for water at 50°C versus 90°C. The net retention time for ethanol in waxy-maize starch only had a threefold reduction (0.046 to 0.014 min) within this temperature range. Also, the highest separation of water at all temperatures was achieved with the waxy-maize starch, which has the highest concentration of amylopectin and demonstrated preferential adsorption for water compared to potato starch, cornstarch, or potato amylose (Rebar et al., 1984).

Neuman et al. (1986) investigated the adsorption characteristics of corn grits at temperatures of 50, 70, 80, and 100°C. Experiments were conducted using a column packed with the corn grit adsorbent. A water-saturated gas stream was passed through the packed column until equilibrium was reached. Equilibrium was determined by measuring the ethanol concentration in the column effluent. The isotherm data was used to find the heat of adsorption. The heat of adsorption (10.8 to 14.6 kcal/g-mol) was in close proximity to the latent heat of condensation (9.7 to 10 kcal/g-mol). This signified a physical adsorption phenomenon (Neuman et al., 1986).

Another type of natural adsorbent is cellulosic-based materials. These include adsorbents such as wheat straw and wood chips. Cellulosic adsorbents rely on the hydroxyl groups of the polysaccharides of the cellulose and the hemicelluloses, Figure 2.3, for binding sites of the water molecule.

Vareli et al. (2000) used inverse gas phase chromatography to determine the adsorption characteristics of wheat flour, a starch based adsorbent, and wheat straw, a cellulosic adsorbent. These studies were conducted at temperatures of 50 to 90°C to calculate the Gibb's free energy and enthalpy of adsorption. See Table 2.2. Also, a study to determine the thermal effects of regeneration on the adsorbent substrate was conducted. Regeneration experiments were conducted using helium at temperatures of 140 and 170°C at a flow rate of 25 mL/min for periods of 12 and 24 hours. Results indicated water to be preferentially adsorbed over ethanol at all temperatures studied and also before and after regeneration of the adsorbent.

Table 2.2. Thermodynamics of Water and Ethanol Adsorption onto Biomass Materials

Source	Adsorbent	$\Delta G°_S$ (Water) kcal/g mole	$\Delta G°_S$ (Ethanol) kcal/g mole	$\Delta H°_S$ (Water) kcal/g mole	$\Delta H°_S$ (Ethanol) kcal/g mole
Rebar, 1984	95% Amylose	-4.59	+0.64	-9.3	-5.64
	Potato Starch	-5.37	-0.52	-11.6	-6.32
	Corn Starch	-5.78	-0.54	-11.1	-6.76
	Waxy Maize Starch	-6.36	-0.19	-13.7	-6.30
Vareli, 1997	Cornmeal	-17.90	-2.05	-30.2	-14.3

Table 2.2. Contiuned

Source	Adsorbent	$\Delta G°_S$ (Water) kcal/g mole	$\Delta G°_S$ (Ethanol) kcal/g mole	$\Delta H°_S$ (Water) kcal/g mole	$\Delta H°_S$ (Ethanol) kcal/g mole
Vareli, 1997	Wheat Flour 70%	-21.05	-3.77	-43.2	-15.8
	Wheat Flour 85%	-19.79	-3.35	-40.8	-15.9
	Wholemeal Wheat Flour	-22.12	-5.31	-46.2	-20.2
Vareli, 1997	Soy Flour	-19.12	-4.52	-38.8	-16.6
	Pine Sawdust	-20.50	-7.03	-43.9	-18.4
Vareli, 1998	Wheat Straw	-22.30	-4.85	-50.0	-15.1

It was found that, after thermal regeneration, the adsorbent's affinity to water decreased at 140°C and decreased even more at 170°C for both materials. This was explained by the possibility of both physical and chemical changes occurring within the structure of the biomass material when heated to temperatures of greater than 100°C. These physical changes would result in a decrease in the accessibility of the hydroxyl groups due to a change in the crystallinity of the cellulose. The chemical changes result in the altering of the heteroxylans to furfurals, which are less hygroscopic towards water (Vareli et al., 2000).

Carmo and Gubulin (1997) studied the thermodynamic and kinetic behavior of starchy materials in the liquid-phase ethanol/ water system. The starch adsorbent used in this study was manioc pellets, which are the precursors to tapioca. In a thermostated bath, thermodynamic data were obtained at temperatures of 25, 40, 50, and 60°C, while kinetic data were obtained using a recirculating liquid bath cell. Manioc pellets were found to have an affinity for water in the presence of ethanol with an adsorptive capacity in the proportion of 15% of its dry mass at 25°C, decreasing with increasing temperature. The Chakravarti isotherm proved to adequately represent the isotherm data.

The kinetic results were dependent upon the variables studied, which were temperature, interstitial velocity, and particle diameter. The results indicated that an increase in temperature provoked an increase in the adsorption rate, but it decreased the capacity to retain water for long periods. Also, the external resistance to mass transfer decreases with an increase in interstitial velocity to the point that the liquid film surrounding the particle became extremely thin. In addition, a decrease in the adsorption rate is seen with an increase in the mean particle diameter of the manioc pellet, but diffusivity values remain largely unaffected. The manioc starch showed a smaller adsorption capacity and lower adsorption rates when compared to 3-Angstrom molecular sieves, for all temperatures considered (Carmo and Gubulin, 1997).

Beery and Ladisch (2001), in a kinetically controlled experiment, studied the effects of increasing water concentration on the adsorptive capacity of starch-based adsorbents for liquid-phase ethanol/water mixtures. The method consisted of contacting dried adsorbents with different concentrations of ethanol/ water mixtures. The

concentrations studied were 1, 2.5, 4.5, and 20 wt% water. The adsorbent and the mixture were placed in a test tube and then mixed with a vortex mixer for 10 minutes.

The results indicate that the mass of water adsorbed increased as the water content increased from 1 to 20 wt% water. For molecular sieves, the mass of water adsorbed increased only up to 4.5 wt% water and then decreases. The conclusion drawn from the starch-based adsorbents was that the water molecules would increasingly find available hydroxyl group adsorption sites as the number of water molecules per unit volume increased. This leads to a higher driving force for adsorption. The molecular sieves, on the other hand, entrap water in pore spaces having dimensions that match the steric characteristics of the water. Therefore, steric hindrances could prevent proper internal adsorption at higher water loadings (Beery and Ladisch, 2001).

In order to fully comprehend the adsorption phenomenon, a closer look at the adsorbent surface is necessary. The major constituents of cellulosic adsorbents are cellulose, hemicelluloses, and lignin. According to Svedas (1998), long crystalline microfibrils, within the cellulose matrix, are wound around the fiber axis and form three distinct layers. These microfibrils are joined together through hydrogen bonding and are embedded in an amorphous matrix of hemicellulose (Svedas, 1998). The lignin, which has a complex molecular structure, acts as an adhesive and stiffening agent for the cell walls of the cellulose and hemicellulose (Han and Rowell, 1996).

For maximum water adsorption, it is desirable to find a material that is amorphous with a high concentration of hemicellulose and cellulose (Han, 1998; Svedas, 1998; Czihak et al., 1999). High hemicellulose concentrations are more desirable than high cellulose concentrations. Cellulose is up to 80% crystalline, whereas hemicelluloses are

generally amorphous. A high percentage of xylan, the polymeric form of the sugar xylose, is an indication of high hemicellulose concentrations (Han, 1998). As evident from Figures 2.3 – 2.5**,** there is an abundance of hydroxyl groups stemming from the xylans. These hydroxyl groups provide the necessary hydrogens needed for hydrogen bonding of water molecules. Only the hydroxyls located on the surface are accessible to water sorption molecules (Svedas, 1998).

The hydroxyl group/water interaction is a complex one. As the H_2O molecule is brought into contact with the OH^- group, one water hydrogen becomes the proton donor and the other becomes the proton acceptor. Only the hydroxyls located on the adsorbent surface are available to adsorb water. That is, those that are wound within the inner microfibril matrix are not accessible to the water molecules. The adsorbed molecules of water perturb the surface hydroxyl groups, shifting their vibrations to lower frequencies. The free hydroxyl groups have a shorter wavelength than the disrupted ones (Svedas, 1998).

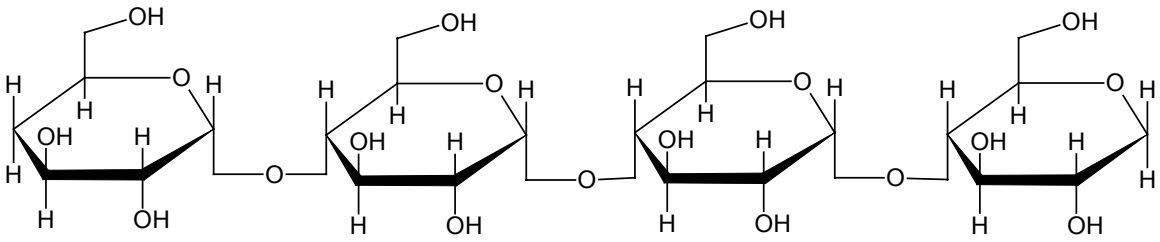

Figure 2.1. Chemical Structure of Amylose

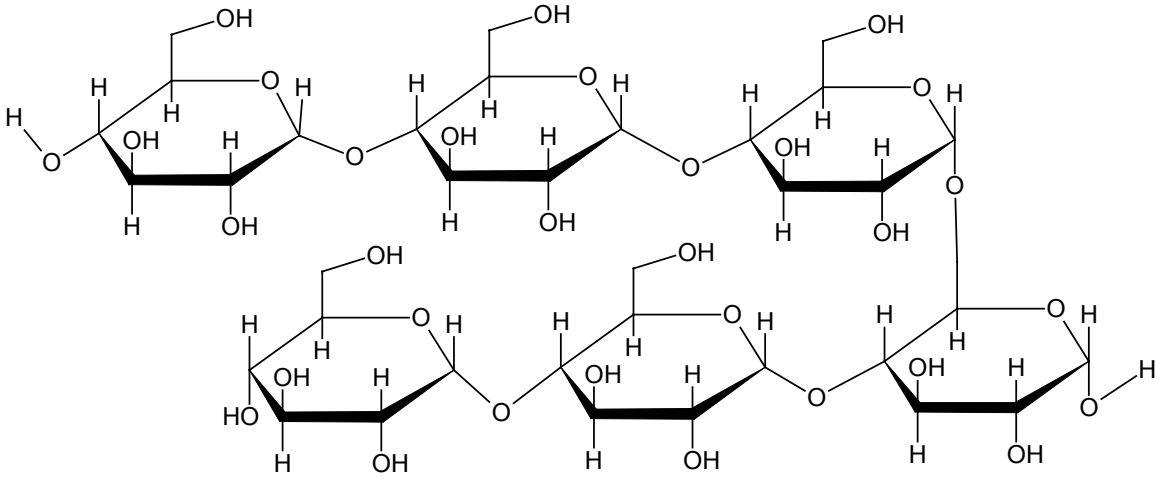

Figure 2.2. Chemical Structure of Amylopectin

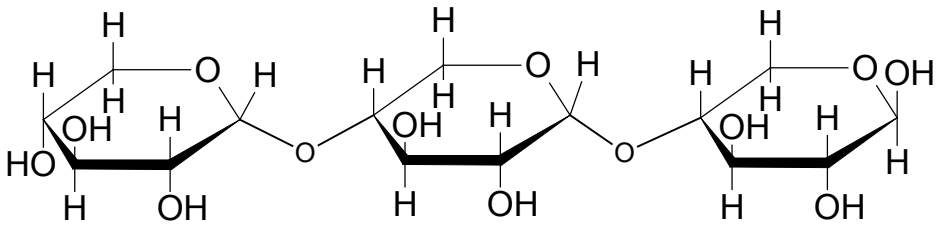

Figure 2.3. Chemical Structure of Xylan

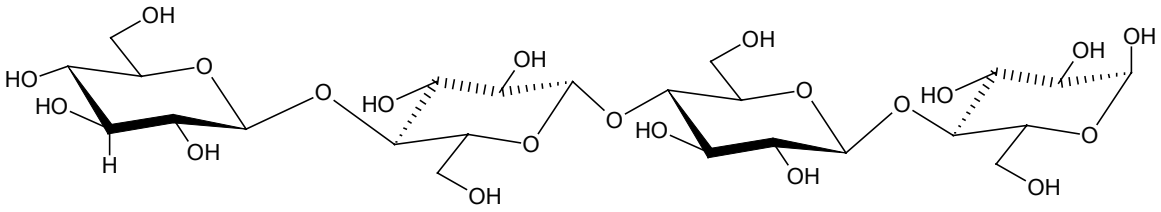

Figure 2.4. Chemical Structure of Cellulose (β-D-glucopyranose)

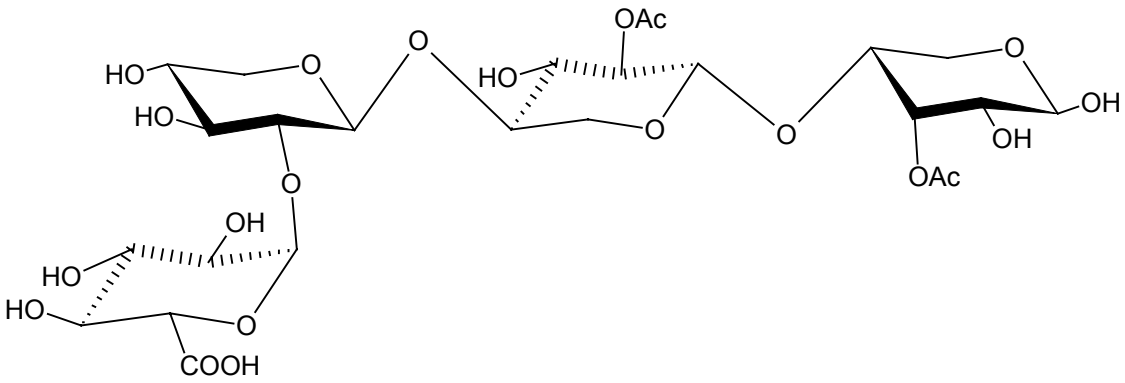

Figure 2.5. Chemical Structure of Hemicellulose (0-Acetyl-4-O-methyl –α –D-glucoronoxylan)

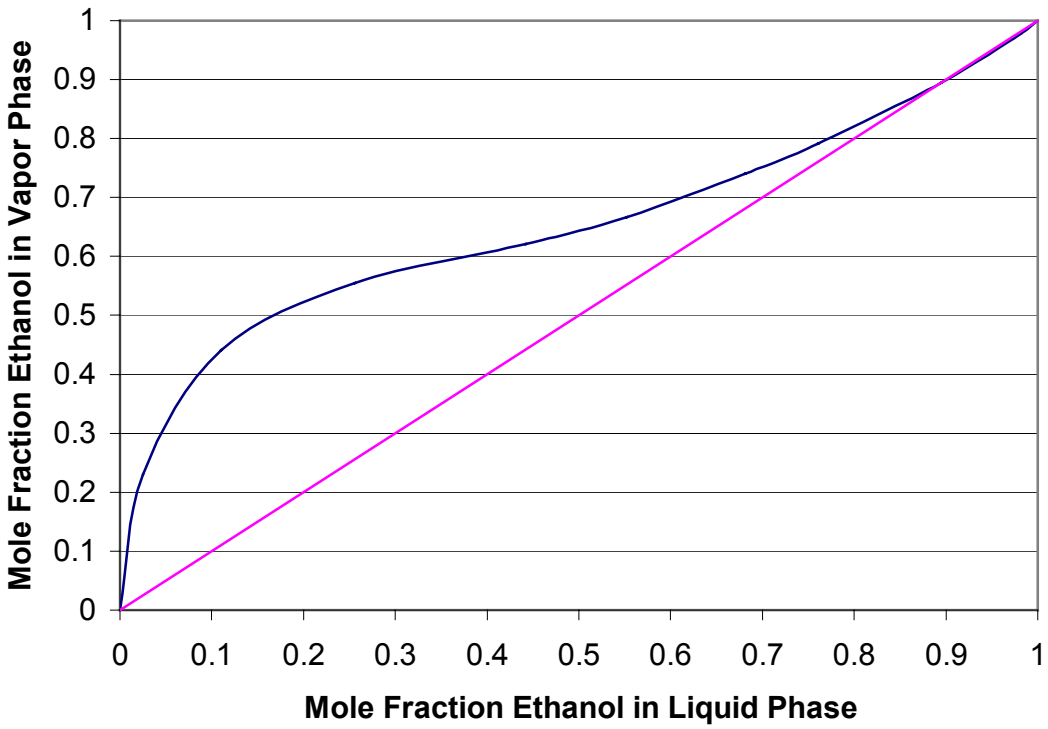

Figure 2.6. Vapor Liquid Equilibrium of Ethanol/Water at 1 atm Pressure

CHAPTER III

THEORY

Background

Adsorption of water from an ethanol/water system has been extensively studied using molecular sieve and starch-based biomass materials; however, little research has been reported on the effect of aqueous ethanol dehydration using cellulosic-based biomass. Also, most studies only examine gas-phase adsorption of water from ethanol, whereas there is only a limited amount of published information using liquid-phase adsorption.

It was found in the laboratory that a system using a cellulosic adsorbent material has a similar effect for the removal of water as a starch-based system. With this encouraging revelation, cellulosic adsorbent materials were investigated using both gas-phase and liquid-phase adsorption systems.

If cellulosic adsorbents demonstrate similar positive effects for the removal of water from ethanol, then they may be better suited for use in adsorptive dehydration systems where starchy adsorbents are not as readily available. To ascertain the relevance of using cellulosic materials, they must perform as well as, if not better than, starchy materials in three main categories. These are: 1) chemical selectivity, 2) adsorptive capacity, and 3) operational column dynamics.

Chemical Selectivity

It is paramount that the adsorbent used in a particular adsorption system adsorb the desired component and reject, or only slightly adsorb, the other components. For the ethanol/ water system, it is desirable to adsorb the water and not the ethanol, providing a product stream that is nearly 100 percent rich in ethanol. To accurately compare the chemical selectivity of adsorbents, a separation factor is defined.

$$\alpha = \frac{X_A Y_B}{Y_A X_B} \tag{3.1}$$

Where:

X_A = Mole fraction of component A in the adsorbed phase

X_B = Mole fraction of component A in the fluid phase

Y_A = Mole fraction of component B in the adsorbed phase

Y_B = Mole fraction of component B in the fluid phase

Maximizing the separation factor is necessary when designing an adsorption system, as the separation factor generally varies with temperature and composition; and therefore, appropriate operating conditions must be chosen with care. For adsorption processes, the mixture component that is selectively adsorbed is the one that is the least resistant to mass transfer, while the other component(s) may be adsorbed to a lesser extent due to increased rates of diffusion into the porous substance. Therefore, an understanding of the diffusion resistances is vital in determining rate-limiting steps. There are two basic types of resistances to mass transfer. First, external resistances are those found between the bulk fluid and the external surface of the adsorbent. Second,

internal resistances hinder the mass transfer of a species from the adsorbent's external surface into its porous matrix (Fogler, 1999).

Molecular Mechanism

To identify the chemical selectivity of an adsorbent, the molecular mechanism by which adsorption takes place must be understood. For example, Type A Molecular Sieves utilize a unique tetrahedral structure of silica and alumina forming pore openings of about 3-Angstroms to adsorb water by molecular size exclusion (Schweitzer, 1996). On the other hand, bio-based adsorbents use intermolecular forces caused by hydrogen bonding and dipole moments as the mechanism to adsorb water molecules. Starch adsorbents contain large percentages of amylopectin, a branched form of glucose, that entrap water molecules with its abundance of hydroxyl groups (Rebar et al., 1984). For cellulosic materials, the binding of water comes mainly from hydroxyl groups that stem from the heteroxylans forming the non-cellulosic polysaccharide portion of the plant cell (Vareli, et al., 1998; Nikitin, 1966).

Intermolecular forces, such as dipole – dipole interactions and hydrogen bonding, interact to form a sense of stability among molecules. They have attractive forces at short ranges, < 1 nm between molecular contact, and repulsive forces, extending up to 100 nm, at long ranges. Dipole – dipole interactions are van der Waals forces and have a binding energy of ~1 kJ/ mol, while hydrogen bonds (binding energy of 10 – 40 kJ/ mol) are electrostatic interactions that exist among molecules that have hydrogen atoms bonded to electronegative atoms such as oxygen, nitrogen, and fluorine (Israelachvili, 1985).

Therefore, hydrogen bonding is primarily responsible for the hygroscopic effect existing between water and the hydroxyl groups found within biomass adsorbents.

Mechanical Mechanism

The mechanical driving force of adsorption results from diffusion due to a concentration gradient, a pressure gradient, or external forces acting unequally on various chemical species. Diffusion by an unsteady state concentration gradient can be depicted from Fick's second law of diffusion.

$$\frac{\partial C_A}{\partial t} = D_{AB}\nabla^2 C_A \qquad (3.2)$$

Where,

C_A = Concentration of species A

t = Time

D_{AB} = Diffusivity of species A into species B

This law states that the rate of change in concentration of species A in a volume element is proportional to the rate of change of the concentration gradient of species A at that point (Bird, et al, 1960).

Adsorptive capacity

The amount of adsorbate that an adsorbent can retain is known as its adsorptive capacity, and the threshold capacity occurs at breakthrough, or saturation, in an adsorption column. The adsorptive capacity of all adsorbents decreases with increasing temperatures, even though the rates of diffusion increase. Also, the adsorption process is always an exothermic one (Schweitzer, 1996). The adsorptive capacity of a substance is

relative to the number and availability of binding sites that occur on the surface of the adsorbent.

Calculated Method

This method is used to calculate the quantity of adsorbed material by the adsorbent. The adsorptive capacity is expressed as in Equation 3.3.

$$q_{ads} = \frac{M_L}{M_A}\left(\frac{C_{f,etoh} - C_{i,etoh}}{C_{f,etoh}}\right) \tag{3.3}$$

Where,

q_{ads} = Mass of water adsorbed per unit mass of adsorbent (g H_2O/g Adsorbent)

M_L = Mass of liquid (g)

M_A = Mass of adsorbent (g)

$C_{f, etoh}$ = Final mass fraction of ethanol in solution

$C_{i, etoh}$ = Initial mass fraction of ethanol in solution

This equation assumes that the adsorbed material is primarily water, not ethanol. This hypothesis is in conjunction with the work of Rebar et al. (1984), in which the chemical affinity of starch to water was shown to be much greater than that of starch to ethanol. The same is also true for cellulosic materials with their high content of xylans (Rebar, et al., 2000).

Graphical Method

A graphical method can be employed to determine an adsorbent's capacity to adsorb water. A graphical representation of data can be made, in which the normalized

concentration of water is plotted versus the total adsorbate volume of the experiment. As shown in Figure 3.1, the total amount adsorbed is the area that exists above the curve. This area is estimated by creating a triangle from the linear portion of the curve up to the point of breakthrough, or threshold (McCabe, et al, 1993). Threshold for the ethanol/ water system is governed by its use as a motor-fuel additive, which is 99.5 wt%.

Equilibrium data obtained from liquid phase adsorption experiments leads to adsorption isotherms that can be modeled mathematically. Modeling is useful in describing the adsorption phenomenon. The use of different adsorption models is necessary depending on the adsorbent, the adsorbate, and the unadsorbed component. Several models have been used for the evaluation of ethanol and water adsorption onto biomass adsorbents. The one proposed for this study was developed by Chakravarti and Dhar (1907).

$$q_{ads} = \frac{q_o\left(K_m C_o\right)^v}{1+\left(K_m C_o\right)^v} \tag{3.4}$$

Where,

q_o = Capacity of the monolayer (g H_2O/g adsorbent)

C_o = Mass fraction of water in the liquid phase at equilibrium

K_m = Chakravarti's constant

ν = Chakravarti's constant

Operational Column Dynamics

The operation of an adsorption column is a dynamic one in which adsorptive capacity is reached at a state of equilibrium. Therefore, traditional thermodynamic

analyses are not applicable as with most chemical separating techniques. The Mass Transfer Zone (MTZ) is the differential volume element within an adsorption column where the concentration gradient is present. As can be seen by Figure 3.2, it starts at the beginning of the adsorbent bed and then moves in the direction of flow as saturation takes place (Crittenden and Thomas, 1998).

The length and velocity of the MTZ are established from the concentration profile of a kinetic adsorption experiment (Schweitzer, 1996). Figure 3.3 illustrates the normalized concentration versus time exhibiting the dynamics of the system. For a symmetrical breakthrough curve, the velocity of the MTZ is found from the time for $C_O/2$ to occur.

$$U = \frac{L}{t} \tag{3.5}$$

where,

U = Velocity of MTZ

L = Length of adsorbent bed

t = time elapsed for the appearance of $C_O/2$

The length of the MTZ, M, can now be determined using Equation 3.6, where Δt is the period of time from the measurement of the initial detectable concentration to the inlet concentration C_O.

$$M = U\Delta t \tag{3.6}$$

Initially, the adsorbate concentration in the fluid decreases from C_O to zero if the adsorbent is at first fully free of the adsorbate (Crittenden and Thomas, 1998). A steep

breakthrough curve indicates an MTZ that is narrow compared to the bed length. If, on the other hand, the breakthrough curve is wide, then the MTZ is almost as long as the bed and less than half of the bed capacity is utilized. It is advantageous to have an MTZ that is narrow to make efficient use of the adsorbent and to reduce regeneration costs (McCabe, et al., 1993).

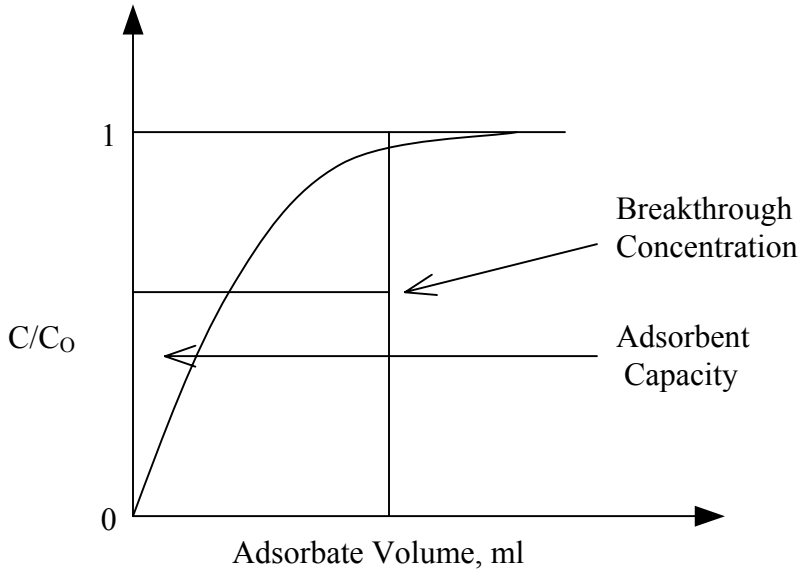

Figure 3.1. Graphical Method for Determining Adsorbent Capacity

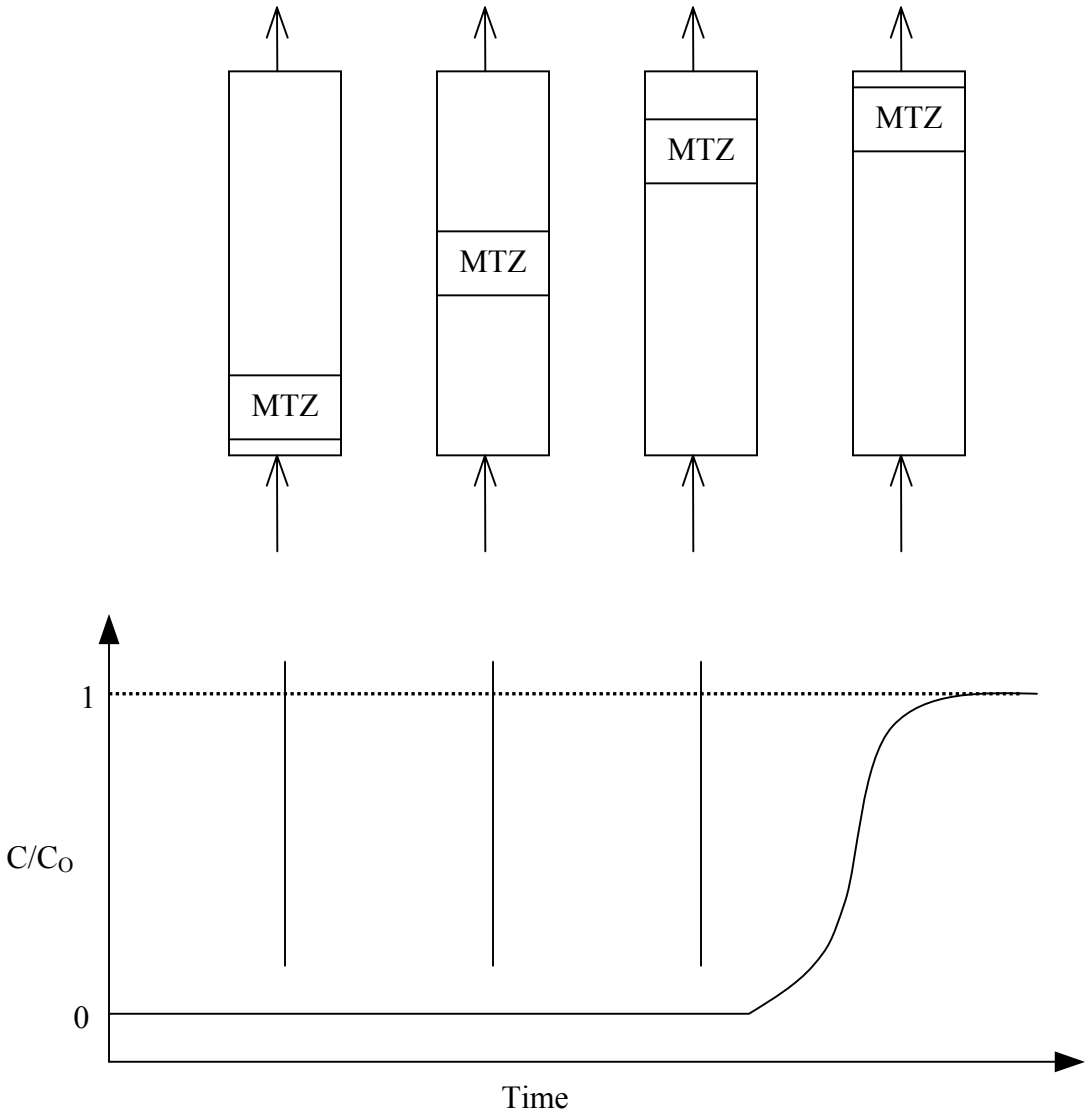

Figure 3.2. Diagram Demonstrating the Relative Relationships Between the Concentration Profile, the Mass Transfer Zone, and the Breakthrough Curve in a Packed Bed Adsorber

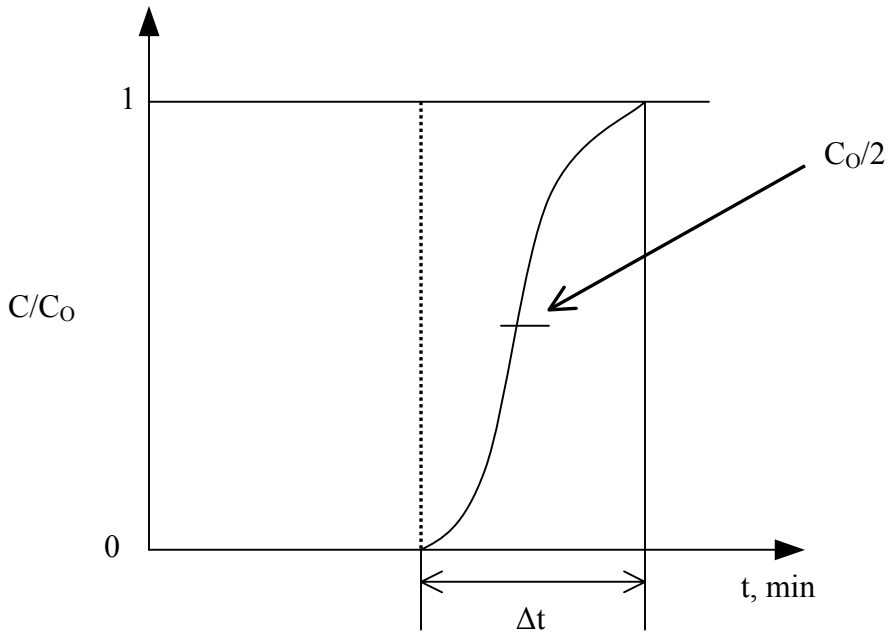

Figure 3.3. Illustration Determining Δt and $C_O/2$ to Find the Velocity and Length of the MTZ

CHAPTER IV

METHODS AND MATERIALS

In this study, cellulosic biomass materials were used to investigate adsorption of water from ethanol/ water mixtures by the liquid phase adsorption method and the gas phase adsorption method. For both methods investigated, a series of batch experiments were conducted to determine equilibrium and operational adsorption characteristics of the adsorbent. Desorption experiments were conducted for the gas phase experiments to reveal operational column characteristics and determine the feasibility of adsorbent reuse in an industrial adsorber.

The adsorbents tested in this study were 3A molecular sieves, bleached wood pulp, hardwood sawdust, and kenaf core. The molecular sieves were used as a test standard because of the abundance of available published information. Once the experimental method and testing procedures had been validated using molecular sieves, attention could then be given to the biomass adsorbents.

Adsorbent Pretreatment

Both, the hardwood sawdust and kenaf core, were sifted and clarified in a pretreatment process. These adsorbents were sifted first in a 40-mesh (0.0130 mm

opening) screen to remove fine particles of material that might swell during operation. A 10-mesh (1.651 mm opening) screen was then used to filter out large particles. These particles may inhibit adsorption by reducing the amount of available surface area, and hence, the amount of available adsorption sites. The adsorbents were then clarified in a pretreatment process to remove any impurities that may reside on the surfaces of the adsorbent particles. Early experimental runs yielded an ethanol product that had an ambered discoloration, indicating that impurities such as resins and tannins were already adsorbed onto the biomass and had leached into the ethanol. These impurities may decrease the number of available sites used for water adsorption. The following pretreatment procedure was thus developed.

1) Place 25 g of material into a 500 ml Erlenmeyer flask.
2) Add enough distilled water to fill flask to 500 ml.
3) Stir mixture allowing the impurities to leach into the water medium.
4) Drain off water and refill with more distilled water.
5) Repeat steps 3 and 4 until the water no longer has a "murky" appearance (about 6 to 8 times during the course of one week).
6) Place adsorbent in a drying oven to dry. Once dry, it is then ready for use.

Oven temperature is critical to proper drying. If the oven temperature is too high, there is a chemical change to the adsorbents. An oven temperature of 90°C was chosen to keep the xylan and glucomannan polymers from changing to furfural polymers. Furfural polymers would be less hygroscopic towards water and would lead to a reduced overall hydrogen bonding capacity of the cell wall. These changes are clearly visible

with bleached wood pulp as it turns from bright white to dingy yellow at temperatures above 100°C.

Gas Phase Column Experiment

A glass column apparatus with a 1.0 L flask was employed to determine the adsorption of water in gas-phase conditions. For the series of gas phase experiments, the experimental setup is sketched in Figure 4.1. A mixture of ethanol and water was heated to produce a vapor stream that traveled upwards into the vacuum jacketed column packed with adsorbent. A column with an inside diameter of 1.0 inch (25 mm) and a length of 30.0 inches (76 cm) was used to provide sufficient column length and an adequate amount of adsorbent material to make dynamic column calculations possible.

The ethanol/ water mixtures were blended using 200-proof ethanol and distilled water. Concentrations of 90, 95, and 97 wt% ethanol were used to evaluate adsorption characteristics at, above, and below the azeotropic concentration of 95.6 wt% ethanol.

A thermal swing desorption system was employed to remove the water from the adsorbent. The experimental procedure used for gas-phase adsorption is as follows:

1) The gas-phase adsorber is assembled as shown in Figure 4.1, except for the collector and condenser.
2) At the bottom of the column, 316 Stainless Steel non-adsorbing packing is added to a height of 1 inch (25 mm) to ensure proper radial distribution of vapors as boil-up occurs.
3) The designated adsorbent is then dumped into the column until the column section is full.

4) The collector and condenser are assembled, leaving the top vented, and the hot air stream is started with a temperature of 85°C and a flow rate of ~4.5 cfh at 1 atm.
5) Once the adsorbent is dry (about 20 hours of hot gas flow), the hot air stream is turned off, the ethanol/ water mixture is added to the 1 L flask, and the flask heater is started using a rheostat to adjust thermal output.
6) As the system heats up to operating temperature, the pressure that builds up inside must be relieved by opening the top sampling port on the collector.
7) Liquid samples are collected after the vapor has traveled through the adsorbent and has been condensed and falls into the collector. Samples are initially taken every 3 minutes for the first 18 to 21 minutes of sample time and then every 5 minutes.

The experimental runs were terminated when the water composition of the condensate equaled that of the feed. This usually took between 45 to 70 minutes, depending upon the adsorbent and the feed composition.

Liquid-Phase Adsorption Experiment

The liquid-phase experiments were conducted using 40 ml glass vials equipped with rubber septa caps to evaluate equilibrium and mass transfer parameters. First, a 2 ml sample of adsorbent was added to a clean dry vial that was then placed in an 80°C oven overnight to thoroughly dry. The vials were removed from the oven, and the caps were immediately screwed onto the vials. A 2 ml portion of an ethanol/water solution was added to the vial through the rubber septa. The vials, containing the adsorbent and the

solution, were then placed onto a wrist shaker and mixed. The experiments were conducted based upon equilibrium conditions.

Materials and Equipment

Water

Distilled water was used throughout the entire project, including the adsorbent pretreatment, gas phase, and liquid phase experiments. Distilled water was used to help eliminate biases that may arrive from impurities that are found in tap water.

Ethanol

Ethanol was obtained from the Mississippi State Chemical Laboratories with a purity of 200-proof. The ethanol was stored in 1 gallon, amber-colored glass bottles. Careful attention was provided to ensure that atmospheric moisture did not contaminate the 200-proof ethanol. This was done by removing the cap, quickly the drawing desired amount from the bottle, and replacing the cap.

Molecular Sieves

The molecular sieves used were 3A molecular sieves purchased from Sigma Aldrich Chemical Supply Company, Inc. These molecular sieves are alumina-silicalite with a tetrahedral crystalline structure. The size distribution of the particles is 8 – 12 mesh with a bulk density of 0.85 g/ml.

Bleached Wood Pulp

Georgia Pacific Corporation supplied the bleached wood pulp used in this study. Bleached wood pulp is a product of the pulping process with the lignin removed. Lignin has an extremely low capacity to adsorb water, and therefore, is a non-adsorbing material in an adsorber. The wood pulp was delivered in 10 X 11.5 inch (25 X 28 cm) sheets. The sheets were shredded and placed into a blender filled with water. After blending, the excess water was strained, and the pulp was allowed to dry, forming small spherically shaped particles. The particles were sieved to remove fine particles (< 18 mesh) and to give a consistent particle size distribution.

Hardwood Sawdust

The hardwood sawdust was supplied by Dewberry Sawmill in Maben, Mississippi. The sawdust was gathered in a 20 L plastic bucket and allowed to cure for about 3 months in open-air atmosphere. Before using in an experiment, the sawdust was sifted and pretreated as described previously. The bulk density was measured to be 0.207 g/cm^3.

Kenaf Core

The kenaf core that was used in this study was purchased from KenGro Corporation in Charleston, MS. It was pretreated before using and was sifted to remove particle sizes less than 18 mesh. It has a measured bulk density of 0.094 g/cm^3.

Gas Chromatograph (GC)

A gas chromatograph (Model # 6890N) was purchased from Agilent Technologies. It uses an Innowax capillary column with a Flame Ionization Detector (FID) to determine concentration amounts of ethanol. The GC uses Helium as the carrier gas as well as hydrogen and air for the FID. All gases were of the Ultra High Purity grade.

Oven

The oven used to dry the liquid cell experiments was an Isotemp Oven from Fisher Scientific. It has a temperature range from 20 to 220°C and uses gravity flow convection for even drying of specimens. Drying of biomass adsorbents was performed at 80 to 90°C. Temperatures in excess of 100°C may result in degradation of lignocellulosic adsorbents.

Quality Assurance and Control Plan

The gas chromatograph was first calibrated using a set of standards that were carefully prepared in the laboratory. This set of standards included the range of ethanol that was to be expected from the experimental outcome. After the initial calibration, the standard solutions were tested approximately twice a month to ensure proper operation of the GC.

Data Quality

Precision, completeness, and randomization are the three attributes that characterize data quality. Precision is estimated by use of the sample standard deviation. Calculation of the sample standard deviation is performed by the equation:

$$s = \sqrt{\frac{1}{n-1}\sum_{1}^{n}\left(x_i - \bar{x}\right)^2} \qquad (4.1)$$

Experimental completeness is defined as the amount of valid data needed from an experiment to achieve a particular level of confidence resulting from a series of measurements. Completeness is the number of replicates that are required to satisfy the probability, expressed as a percentage. To calculate the number of necessary replicates, n, the formula is expressed as:

$$n = \left[\frac{ts}{CI}\right]^2 \qquad (4.2)$$

CI represents the confidence interval and "ts" is obtained from the "t table." For example, for a 90% confidence interval, the value of "ts" is 1.645, and the value of n approximately equals 3.

Randomization, or allowing "chance" to govern the selection of the sample from the population to be included in the experiment, is paramount to achieving reliable results. Randomization results in a sample being taken in such a way that each sample from the population has an equal chance of being selected. In this study, each biomass adsorbent was stored in a 2-gallon plastic container. This is known as the "population" of the adsorbent. A sample of the adsorbent was then drawn, at random, from the

population. This randomization procedure was carried out for both vapor phase and liquid phase experiments.

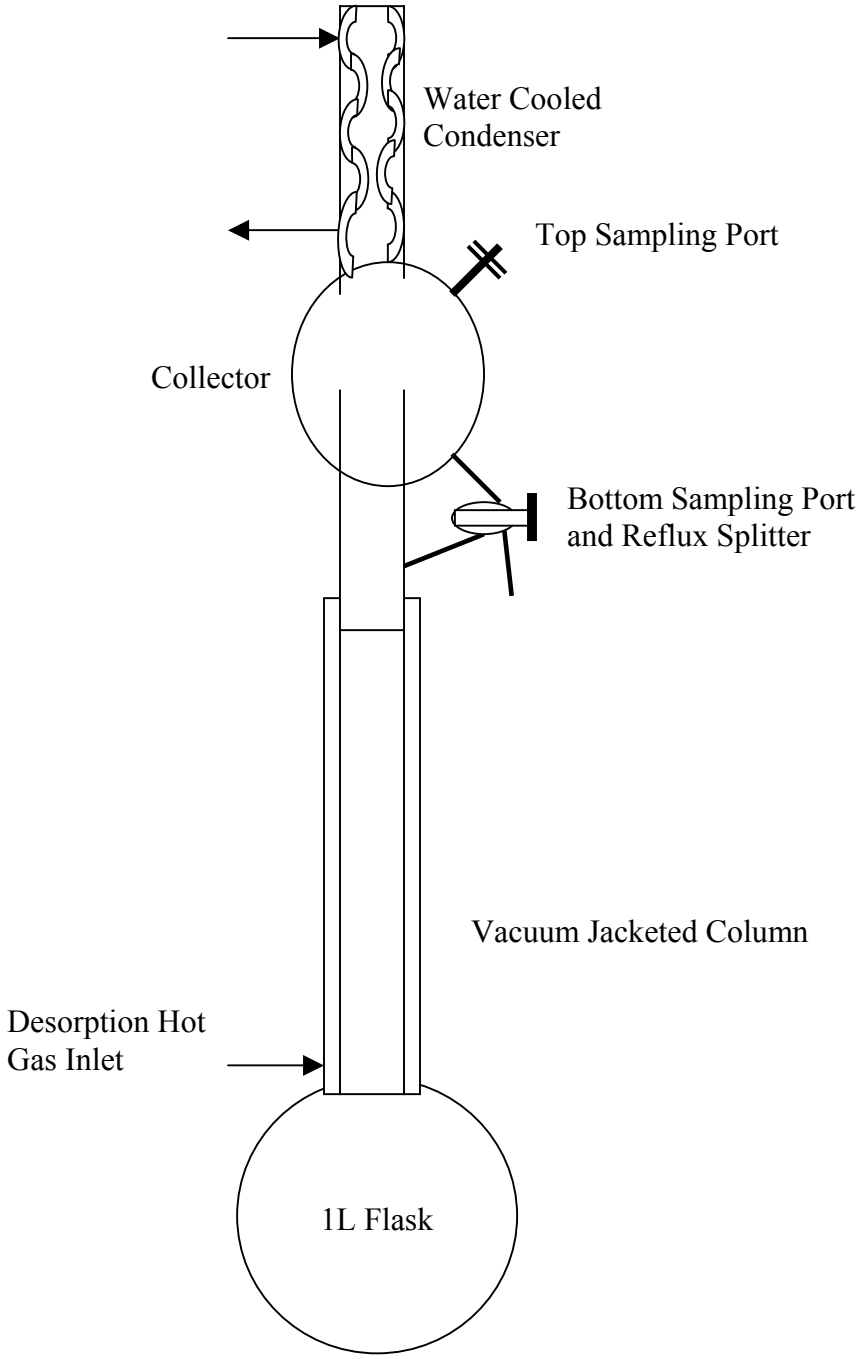

Figure 4.1. Vapor Phase Adsorption Apparatus

Table 4.1. Physical Properties of Ethanol and Water

Property	**Ethanol**	**Water**
Molecular Formula	CH_3CH_2OH	H_20
Molecular Weight	46.07	18.016
Specific Gravity	0.789	1.00
Melting Point (°C)	-112	0
Boiling Point (°C)	78.4	100
Solubility	∞ (in water)	

Table 4.2. Physical Properties of Adsorbents

Adsorbent	Bulk Density (g/cm^3)	Surface Area (m^2/g)
Kenaf Core	0.094	9.989
Bleached Wood Pulp	0.130	8.842
Hardwood Sawdust	0.207	4.907

Table 4.3. Chemical Composition of Adsorbents (percent oven dry basis)

Adsorbent	Cellulose	Hemicellulose	Lignin
Kenaf Core	43	39	18
Bleached Wood Pulp	N/A	N/A	N/A
Hardwood Sawdust	42	27	31

CHAPTER V

RESULTS AND DISCUSSION

The main objective of this research was to study the effects of water adsorption onto biomass adsorbents for the purpose of dehydrating ethanol. By understanding the mechanism by which water adsorbs onto a porous solid material, characterization of the adsorption phenomenon within an industrial adsorber can be better understood. Adsorption of water from an ethanol/water solution using molecular sieves, bleached wood pulp, hardwood sawdust, and kenaf core were investigated in a vapor phase column study. Also, the equilibrium adsorption capacity was studied in a batch liquid test. Additionally, column operating parameters, including length and velocity of the Mass Transfer Zone, and mass transport properties were evaluated.

Liquid Phase Equilibrium Adsorption

At ambient conditions, the adsorption of water from an ethanol/ water mixture was evaluated using 40 ml vials in batch experiments. From these experiments, the adsorptive capacity, in g H_2O/ g adsorbent, and the monolayer capacity were determined.

The adsorption isotherms are shown in Figures 5.1 and 5.2. A nonlinear model was used, represented by the Chakravarti - Dhar isotherm given by Equation 3.4, which

satisfactorily correlated the data. The constants obtained by this equation for each of the adsorbents are listed in Table 5.1. Polymath 5.0, a nonlinear regression solver, was used to estimate the isotherm parameters.

Linearization of the isotherm equation demonstrates the true correlation of the data. The Langmuir isotherm equation was also tested but was found to be a biased model. Figure E.4 shows the results of the linearized plots of the Chakravarti – Dhar equation.

Table 5.1. Values of Thermodynamic Parameters Using the Chakravarti-Dhar Isotherm Equation

Adsorbent	q_o	K_m	ν	R^2
	(g H_20/ g adsorbent)	(equation constant)	(equation constant)	(Statistical Value)
Molecular Sieves	0.097	12.15	0.96	0.96
Bleached Wood Pulp	0.341	17.27	1.55	0.87
Hardwood	0.103	18.83	1.41	0.72
Kenaf Core	0.182	31.897	1.81	0.84
Manioc Starch [1]	0.145	40.16	0.87	-

Notes:
[1]The values for the manioc starch are from experiments conducted by Carmo and Gubulin (1997).

The results showed similar adsorption capacities for the molecular sieves, the hardwood sawdust, and the kenaf core. The mass of water adsorbed per unit mass of adsorbent increases for both the molecular sieves and the cellulosic adsorbents as the water concentration in the ethanol/ water mixture increases from 1 to 10 wt%. These results were anticipated because, as the concentration of water increases, the water molecules would progressively find more and more hydroxyl group adsorption sites as the number of water molecules per unit volume increases. This increase in the concentration gradient leads to a significantly higher driving force.

The bleached wood pulp, on the other hand, demonstrated a significant increase over the other adsorbents in its ability to preferentially adsorb water over ethanol. This is a reasonable outcome. An initial hypothesis was made concerning the use of bleached wood pulp. Since this cellulosic adsorbent has already had the lignin removed, there remain more xylans and glucans per unit volume to adsorb water. It is these polysaccharides, and not the lignin, which contains the abundance of hydroxyl groups for the attachment of the water molecules. The lignin, therefore, only offers added structure and adhesion to the cellulosic mass and contributes very few adsorption sites for water molecules. Furthermore, the mass of water adsorbed per unit mass of bleached wood pulp increases as the water concentration in the ethanol/ water mixture increases from 1 to 10 wt%.

Figure 5.3 demonstrates the individual adsorbent capacities as a function of water concentration for each of the adsorbents tested. This verifies the theory that as the concentration of water increases, the adsorbent capacity also increases until enough water molecules are present to saturate the adsorbent material.

Vapor Phase Column Adsorption

The vapor phase adsorption of water onto biomass materials from an ethanol/ water solution was investigated using a batch operated adsorption still. From these experiments, typical adsorber breakthrough curves were obtained. The breakthrough curves are given such that the y-axis is the normalized concentration, in percent water, and the x-axis gives the time throughout the experimental run. The normalized concentration is the value when the concentration of a sample taken at a particular time, t, is divided by the initial concentration of the mixture fed to the adsorber column. These breakthrough curves are then used to determine dynamic operating conditions such as length and velocity of the mass transfer zone (MTZ). Also, adsorbent capacities and diffusivity values are obtained.

Because there is ample literature concerning the use of molecular sieves for the purpose of dehydrating ethanol, Type A molecular sieves were used to verify proper design and use of the laboratory batch column. Once sufficient runs had been made using the molecular sieves and proper operating adjustments had been made, further experiments were conducted using a variety of biomass adsorbents. Adjustments of the rheostat that operated the heater/ boiler were made to achieve a desired vapor velocity through the column. For the column, which had an inside cross sectional area of 5.07 cm^2, a vapor velocity of 3.29 mm/s was chosen to yield a volumetric flow rate of approximately 1.00 cm^3/min.

Hardwood Sawdust

The hardwood sawdust used in this study was prepared according to the procedure outlined earlier in Chapter 4. Preliminary experimental runs were tried without using a sifting procedure. Fine dust particles created a "clogging" effect within the column. This produced a large pressure drop across the adsorbent bed causing column flooding to occur. After removal of the dust-size particles, column flooding did not occur.

A photomicrograph was taken of the hardwood sawdust and can be seen in Figure A.1. From this micrograph, one can see the porous structure that provides access to the water adsorption sites. Figures 5.4 – 5.6 illustrate that hardwood sawdust had longer breakthrough times than the kenaf core and the bleached wood pulp. The vapor flow rate of the hardwood, less than 1.00 ml/min, was the smallest of all the adsorbents. The hardwood sawdust had the highest column packing density with 51.9 g of adsorbent placed in a volume of 451 cm^3.

An interesting observation in the experiments using hardwood sawdust is that the liquid removed from the boiler flask, which was initially clear in appearance, had a brown to amber color. This discoloration came from extractables that leached from the woodchips into the ethanol/ water mixture.

These extractables were not removed during the clarification stage because heat, which is necessary to remove the extractables from the woodchips, had not been added to the woodchips/ water mixture. Furthermore, the color of the liquid from the boil up flask appeared to be darkest from Runs 2 and 3 and then began to get lighter in color with each successive run. This occurred since there is a lower concentration of extractables with each succeeding run. At any rate, this removal of extractables did not appear to have any effect on the woodchips' capacity to adsorb water. That is, the data did not show any

increase or decrease in amounts of water adsorbed with respect to time from one run to the next.

Bleached Wood Pulp

The bleached wood pulp used in this experiment was supplied in a commercially available, flat sheet form that had to be repulped using a blender and water. After drying, the adsorbent was ready for use in the adsorption column. The photomicrographs for the bleached wood pulp are in Figures A.2 and A.3. These photomicrographs demonstrate the change in surface morphology of hardwood after the Kraft pulping process. This adsorbent does not have a porous matrix, but it has a fibrous surface structure with an abundance of hydroxyl groups needed for hydrogen bonding of water molecules.

As can be seen from Figure 5.7, the bleached wood pulp preferentially adsorbed water over ethanol in ethanol/ water solutions of 3, 5, and 10 weight percent water. As expected, the adsorber column yielded longer run times with decreased concentrations of water. That is, column adsorption capacity was reached faster using a solution with a higher concentration of water.

An important consideration with the bleached wood pulp is that it has an increasing ability to swell inside the column with increasing concentrations of water. The adsorbent swelling causes a significant pressure drop across the adsorber. This, in turn, results in column flooding and poor mass transfer of water from the fluid to the adsorbent. The swelling is due to the lack of lignin within the structure of the cellulosic material. It is the lignin that gives the adsorbent rigidity. It acts as a glue to hold cellulose and hemicellulose molecules together. Without the lignin, the adsorbent, on a

per weight basis, has a higher capacity to adsorb water; however, the swelling effect is counter-productive in an adsorber column.

Kenaf Core

The kenaf core also underwent the pretreatment process as prescribed in Chapter 4. The kenaf core was also sifted to remove dust-size particles. The porous structure of the material can be seen in the photomicrographs in Figures A.4 and A.5.

As can be seen from Figures 5.4 – 5.6, the kenaf core had the shortest breakthrough time of the three cellulosic materials. There are several reasons for this. First, compared to the hardwood sawdust, a higher vapor flow rate was obtained resulting in more water per unit time which come into contact with the adsorbent. Also, its bulk density is only about one-half that of the hardwood sawdust. Therefore, fewer grams of adsorbent can be placed inside the adsorption column, leaving less surface area, per unit volume, for adsorption to occur. Secondly, compared to the bleached wood pulp, there are fewer polysaccharides, per unit mass, which provide the hydroxyl groups needed to adsorp the water molecules.

Comparison of Adsorbents

From the liquid phase adsorption experiments, which were conducted on an equilibrium basis, it was believed that the bleached wood pulp would offer the highest ability to adsorb water, followed by the kenaf core, and finally hardwood chips. This, however, was not the case in the column adsorption experiments. While the bleached wood pulp may adsorb more water on a per weight basis, its bulk density is much less than the kenaf core or the hardwood chips. This results in fewer grams of adsorbent that

are actually placed within the column. The same is also true with the kenaf core as compared to the hardwood chips.

Figures 5.7 – 5.9 demonstrate the hygroscopic nature of the adsorbents. As the concentration of water increases, shorter breakthrough times occur. This is because more water has been added to the system, and therefore, the adsorbent reaches its capacity quicker. The experiments conducted at the 95 wt% ethanol level prove that the ethanol can be purified past its azeotropic point. The experiments conducted at the 90 wt% ethanol level demonstrate the possibility of operating an industrial adsorption column in which the feed is somewhat below the azeotropic point. The actual amounts of material placed inside the column with a bed depth of 90 cm are 30.8, 22.4, and 51.8 g of bleached wood pulp, kenaf core, and hardwood chips, respectively. It is possible forcibly pack more of the adsorbent inside the column, but this creates a larger pressure drop inside the column, thereby affecting adequate vapor flow through the column. The relative amounts placed in the column were chosen to offer the best adsorption results with the optimal column operating parameters. This included careful consideration to column flooding caused by too large of a pressure drop across the adsorbent material, especially as the lignocellulosic adsorbent swells.

Another interesting phenomenon to note in the breakthrough curves is the peaks and valleys in the data. After adsorption equilibrium was reached, Figures 5.4 through 5.6 demonstrate a large variability of water content between samples. Also, in nearly all experiments, the concentration of the samples is less concentrated in water at the end of the run than the initial concentration of the feed. This was not expected. It would be reasonable to assume that the concentration of the samples taken at the end of the

experiment would be the same at the end of the experimental run as the initial concentration of the mixture in the boil-up flask. The explanation for this outcome is partial fractionation of the ethanol/ water mixture. Once equilibrium has occurred, there exists a small window of vapor – liquid equilibrium in which the adsorption column performs essentially as a packed distillation column.

Table 5.2 gives the conditions and the results of the breakthrough behavior from the vapor phase column experiments. This table gives breakthrough information for each adsorbent at each of the ethanol/ water inlet compositions. Breakthrough time is defined by the amount of time elapsed from the time of initial sampling until the breakthrough concentration has been reached.

Table 5.2. Conditions and Results for Vapor Phase Column Experiments

Adsorbent	Inlet Composition (mass Fraction Ethanol)	Vapor Flow Rate (ml/min)	Breakthrough Time (min)[1,2]	Water Adsorbed (g)	Water Loading[3]	Water Adsorption Rate[4]
Hardwood	0.97	0.655	14.5	0.285	0.0052	3.786
Hardwood	0.95	0.795	3	0.119	0.0022	0.7660
Hardwood	0.90	0.766	-	-	-	-
Kenaf Core	0.97	0.953	7	0.200	0.0089	1.2758
Kenaf Core	0.95	0.942	3	0.141	0.0063	2.1017

Table 5.2. (Continued)

Adsorbent	Inlet Composition (mass Fraction Ethanol)	Vapor Flow Rate (ml/min)	Breakthrough Time (min)[1,2]	Water Adsorbed (g)	Water Loading[3]	Water Adsorption Rate[4]
Kenaf Core	0.90	1.010	-	-	-	-
Bleached Wood Pulp	0.97	0.989	13	0.3857	0.0125	0.9622
Bleached Wood Pulp	0.95	1.019	7	0.3567	0.0116	1.6524
Bleached Wood Pulp	0.90	0.855	-	-	-	-

Notes:
[1]Breakthrough occurs at an exiting concentration of 99.5 wt% Ethanol.
[2] Values for the breakthrough behavior of 90 wt% ethanol were not obtainable due to insufficient column length.
[3]Water Loading is given by grams H_2O adsorbed per gram adsorbent (g H_2O/ g ads).
[4]Water Adsorption Rate is given by grams H_2O adsorbed per kilogram adsorbent per minute (g H_2O/ Kg ads/ min).

Significance of Adsorbent Properties

Adsorption is a surface phenomenon, and the binding of water to an adsorbent is therefore occurring at the surface. The major constituents of cellulosic-based adsorbents are cellulose, hemicellulose, and lignin. The cellulose is composed of a moderately crystalline matrix with long microfibrils that are wound around a fiber axis. The microfibrils are joined together through hydrogen bonding and are embedded within an amorphous medium of hemicellulose. The lignin acts as a glue to hold together the other components and stiffens the cell walls.

When designing an adsorber to remove water from a mixture of ethanol and water, it is desired to find an adsorbent that is amorphous rather than crystalline. Crystalline structures have a highly ordered molecular arrangement and leave little room for additional molecules to be added. Cellulose has a high degree of crystallinity, up to 80%, whereas, hemicelluloses is essentially amorphous. The lignin, on the other hand, adds very little to the water adsorption quality.

The interactions between molecules of water and the hydroxyl groups attached to the polysaccharides are rather involved. As the H_2O molecule is brought into contact with the OH^- group, one of the hydrogen's of the H_2O molecule becomes the proton donor, and the other hydrogen becomes the proton acceptor. Only the hydroxyls located on the adsorbent surface are available to water adsorption. That is, those that are wound within the inner microfibril matrix are not accessible to water molecules. The adsorbed molecules of water perturb the surface OH^- groups creating shifts of their vibrations to

lower frequencies. The free OH^- groups have a shorter wavelength than the disrupted ones.

Therefore, a material such as bleached wood pulp is theoretically ideal because the lignin has been removed and it is an amorphous material with a high concentration of xylans. Experimentally, however, it does have its drawbacks. Without the lignin, there is no adhesion between cell walls to give the material a rigid structure. Consequently, the fibers swell with the adsorption of water providing a significant pressure drop inside the column adsorber between the boil-up flask and the condenser. This reduces the vapor flow and results in an unsteady state of water adsorption. Without upward vapor flow, the fluid inside the column condenses to a liquid and adsorption ceases to occur.

The kenaf core is considered a non-wood fiber and has a lignin content of 18%. As the lignin content increases, the cellulose and hemicellulose contents decrease. As a result, fewer hydroxyl groups are available and fewer water molecules are adsorbed. It also has a higher concentration of xylans, on a per weight basis, than the hardwood sawdust.

Mass Transfer Characteristics

Figures 5.10 and 5.11 give the amount of water adsorbed by each adsorbent. Breakthrough time is defined as being the time at which the ethanol concentration of the sample is less than 99.5 wt% ethanol. As only the experiments conducted at the 95 and 97 wt% ethanol concentrations yielded results within this specification, only results taken from these concentrations can be used to determine the water loading at breakthrough. It

is concluded that the bleached wood pulp adsorbed more water more quickly than the other two adsorbents, as shown in Figure 5.10.

It is important to note that the hardwood sawdust yielded the longest breakthrough time but had the lowest amount of adsorbed water. This is because experimental runs for hardwood sawdust witnessed the smallest vapor flow rates. This, in turn, means less water per unit time flowed through the column.

Figure 5.11 demonstrates the adsorbents' ability to adsorb water to the point of equilibrium. Equilibrium is characterized as the time when the breakthrough curve develops a plateau, indicating that no more water is being adsorbed. It is concluded that the bleached wood pulp adsorbs more water at equilibrium than hardwood sawdust or kenaf core. These results were expected from the outcome of the liquid phase equilibrium experiments.

Table 5.3. Equilibrium Moisture Content of Each Adsorbent

Adsorbent	Inlet Composition (wt frac etoh)	Vapor Flow Rate (ml/min)	Time for Equilibrium (min)	Water Adsorbed (g)	Water Adsorbed (g H_2O/ g Ads)
Hardwood	0.97	0.655	37	0.727	0.014
Hardwood	0.95	0.795	28	1.113	0.021
Hardwood	0.90	0.766	28	2.145	0.041
Kenaf Core	0.97	0.953	25	0.715	0.032
Kenaf Core	0.95	0.942	20	0.942	0.042
Kenaf core	0.90	1.010	15	1.515	0.068

Table 5.3. (Continued)

Adsorbent	Inlet Composition (wt frac etoh)	Vapor Flow Rate (ml/min)	Time for Equilibrium (min)	Water Adsorbed (g)	Water Adsorbed (g H_2O/ g Ads)
Bleached Wood Pulp	0.97	0.989	36	1.068	0.035
Bleached Wood Pulp	0.95	1.019	30	1.529	0.050
Bleached Wood Pulp	0.90	0.855	27	2.309	0.075

Mass Transfer Zone Properties

From the results of the breakthrough curves, the dynamic characteristics of the Mass Transfer Zone (MTZ) can be calculated. Table 5.3 summarizes the values of the parameters of the MTZ as well as the values of the length and velocity of the MTZ. As discussed in Chapter 3, the MTZ is an integral part in designing adsorption columns. Only experiments conducted at the 95 and 97 wt% ethanol were used to calculate MTZ properties. Experimental results from the 90 wt% ethanol lacked sufficient column height, and therefore, adsorbent volume to produce the necessary data for calculation of MTZ properties.

Table 5.4. Parameters and Characteristics of the Mass Transfer Zone

Adsorbent	Inlet Composition (wt frac etoh)	Length of Bed (cm)	Time Co/2 Occurrence (min)	Δt (min)	Velocity of MTZ (cm/min)	MTZ Length (cm)
Hardwood	0.97	89	24	23.0	3.71	85.3
Hardwood	0.95	89	14	47.5	6.36	302.0
Kenaf Core	0.97	89	19.0	36.5	4.68	171.0
Kenaf Core	0.95	89	12.0	33.0	7.42	244
Bleached Wood Pulp	0.97	89	28.5	24.0	3.12	74.9
Bleached Wood Pulp	0.95	89	37.5	41.0	2.37	97.3

From these results, there is evidence to suggest that feed concentration is a significant variable for the length and velocity of the MTZ. For the hardwood sawdust and the kenaf core, there is an appreciable increase in the MTZ characteristics. For the bleached wood pulp, however, there is only a slight increase in the length of the MTZ and a decrease in the velocity of the MTZ with an increase in feed water concentration. With only two data points, it is unclear whether this is a trend or an anomaly within the data. All of this data is consistent with the experimental results obtained by Crittenden and Sowerby (1990) when ethanol was dehydrated using molecular sieves.

Microscopic Mass Transfer Characteristics

An analysis was performed to determine the true diffusion characteristics occurring at the surface of the adsorbents. The external mass transfer coefficient can be used to help explain the behavior of adsorption systems. Two different correlations were used to ascertain the external mass transfer coefficient of each adsorbent at each concentration level of ethanol. These correlations were the Colburn J Factor Correlation and the Thoenes – Kramers Correlation. These data are represented in Figure 5.12.

The values calculated from the Colburn J Factor were larger than the ones calculated from the Thoenes – Kramers correlation. In the case of the bleached wood pulp, these values were significantly higher. These differences arise mainly from the dependence of the Reynolds Number on the Colburn J Factor. This correlation is used for a wide range of particle shapes and sizes and varying vapor flow conditions.

In general, the external mass transfer coefficient is largest for the bleached wood pulp, followed by the kenaf core, and then the hardwood. This leads to an explanation for the trends seen from Figures 5.10 and 5.11. The bleached wood pulp, which had the highest amounts of water adsorption capacity, also has the highest mass transfer coefficient. This results in a larger molar flux resulting in more molecules per time arriving at the particles' interior surfaces.

As an additional qualitative approach to explain adsorption behavior, the surface area of the adsorbents was measured. The larger the surface area, the more hydroxyl rich xylans than can be accessible for the securing of the water molecules to the adsorbent. As can be seen from Figure 5.13, the kenaf core had the largest surface area, followed by the bleached wood pulp and then the hardwood sawdust. This would automatically lead

to the conclusion that kenaf core should have a higher adsorption capacity. This would be true except that the bleached wood pulp has a higher concentration of xylan due to the lack of lignin in its makeup.

Pressure Swing Adsorption Experiments

Although the main focus of this experimental work was centered on thermal swing adsorption, some experimental work was performed using pressure swing adsorption (PSA). In PSA, the adsorption step is carried out at a higher pressure (usually at 100 psia) than the desorption step (14.7 psia). In this manner, when the adsorption capacity has been reached, the column pressure is lower allowing for desorption of the adsorbate and it can be removed from the column.

The PSA experiments were performed using the same glass column, boiler, and condenser as the TSA experiments. Inasmuch, it was believed that a high pressure of 100 psia would be enough to burst the equipment. Therefore, the adsorption step was run at atmospheric pressure just as the TSA experiments. The desorption step, however, was carried out using a vacuum pump that repeatedly pumped down to a pressure of 29.5 inches of mercury. In this manner, a simulation of PSA could be attempted.

Results from the PSA experiments indicated that less than one hundred percent of the moisture was removed. The results, therefore, were not encouraging. Each adsorbent was tested by first running an adsorption experiment and then using the vacuum pump to remove the moisture inside the column. The vacuum was allowed to run until a pressure of 29.5 in Hg had been maintained for at least 5 hours. The data collected from these experiments did not show that water had been removed from the ethanol/ water system.

An assessment was made to determine the cause of these results. A moisture content analysis was made on the adsorbents after an adsorption/ desorption cycle. On average, the moisture content of the adsorbents after vacuum desorption ranged between 5 and 8% moisture. It is believed that this moisture content is too high for the adsorbent to be effective in removing water from an ethanol/ water mixture.

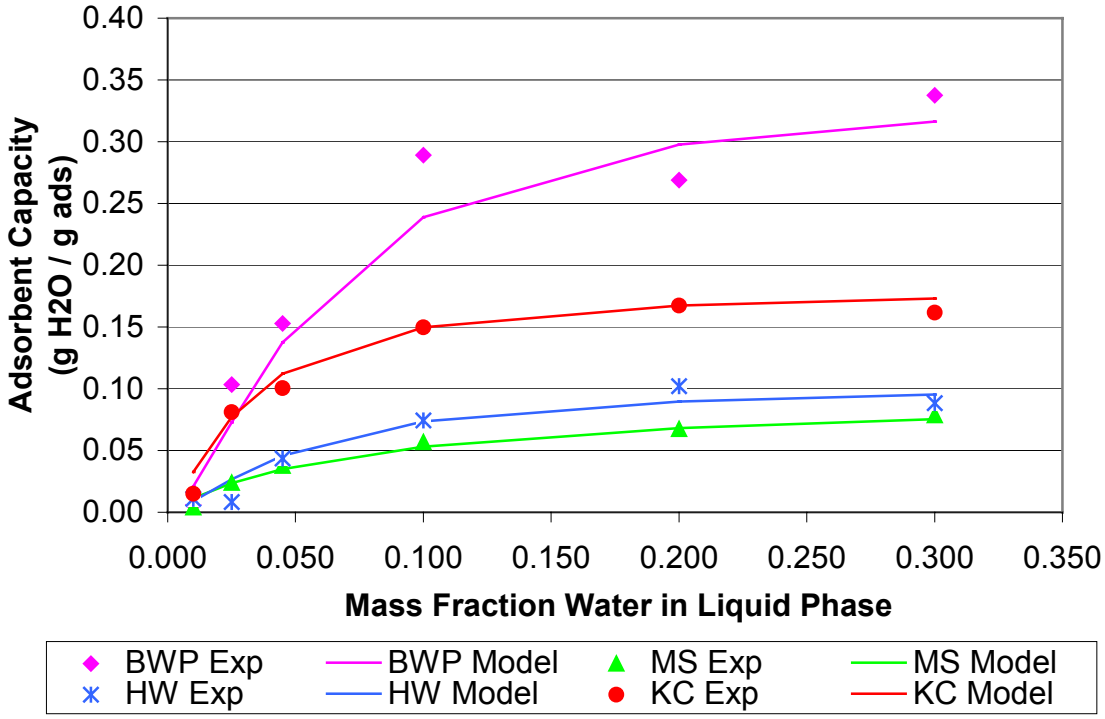

Figure 5.1. Liquid Phase Equilibrium Adsorption Isotherms at Ambient Conditions

Note: The points are from actual data, while the lines are from the Chakravarti-Dhar isotherm equation.

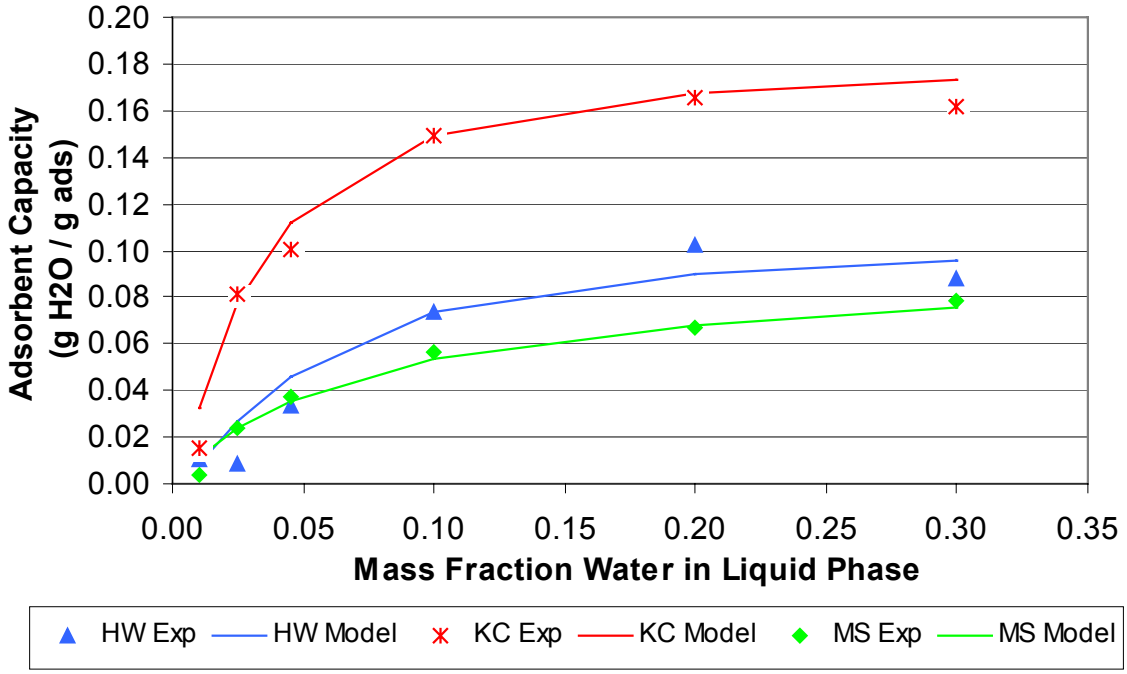

Figure 5.2. Liquid Phase Equilibrium Adsorption Isotherms at Ambient Conditions Without the Bleached Wood Pulp (for emphasis purposes)

Note: The points are from actual data, while the lines are from the Chakravarti-Dhar isotherm equation.

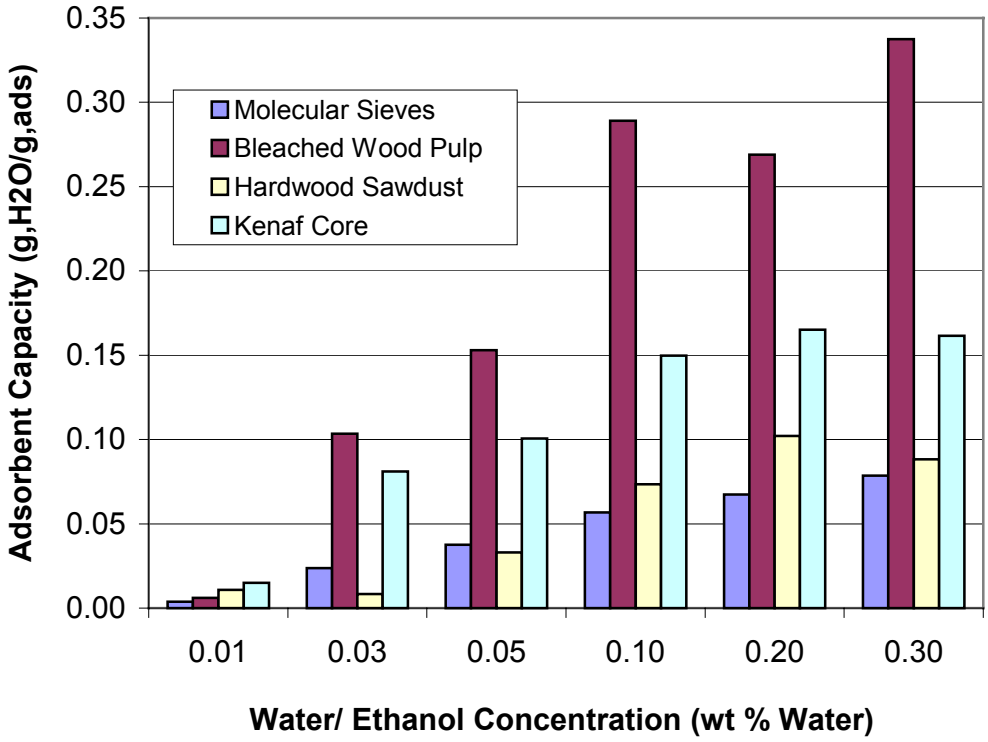

Figure 5.3. Liquid Phase Equilibrium Adsorption Isotherms at Ambient Conditions Demonstrating the Increase of Adsorption with the Increase of Water Concentration

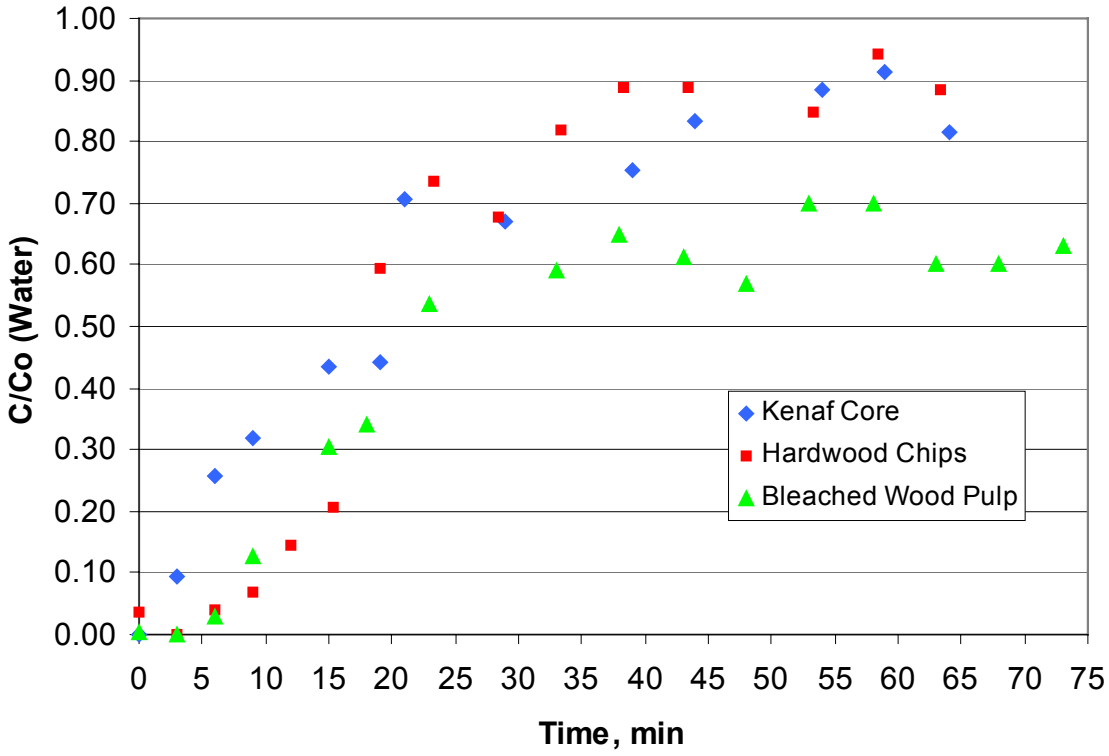

Figure 5.4. Breakthrough Curves Comparing the Capacities of the Adsorbents at an Initial Feed of 97 wt% Ethanol

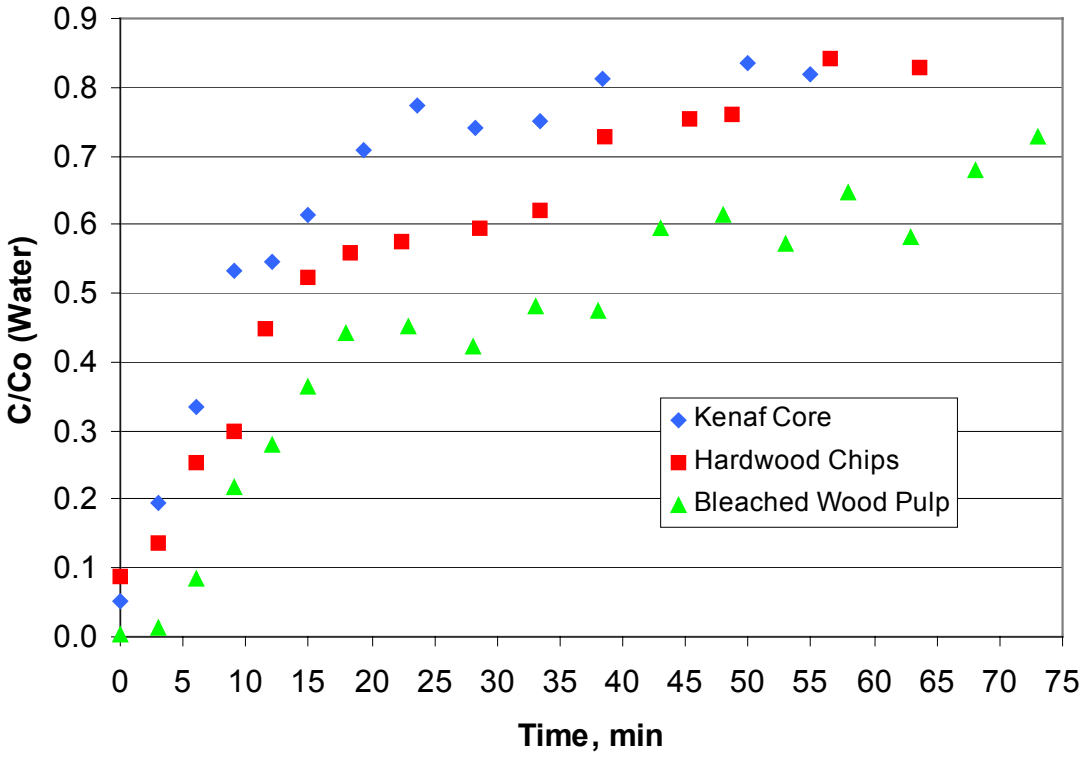

Figure 5.5. Breakthrough Curves Comparing the Capacities of the Adsorbents at an Initial Feed of 95 wt% Ethanol

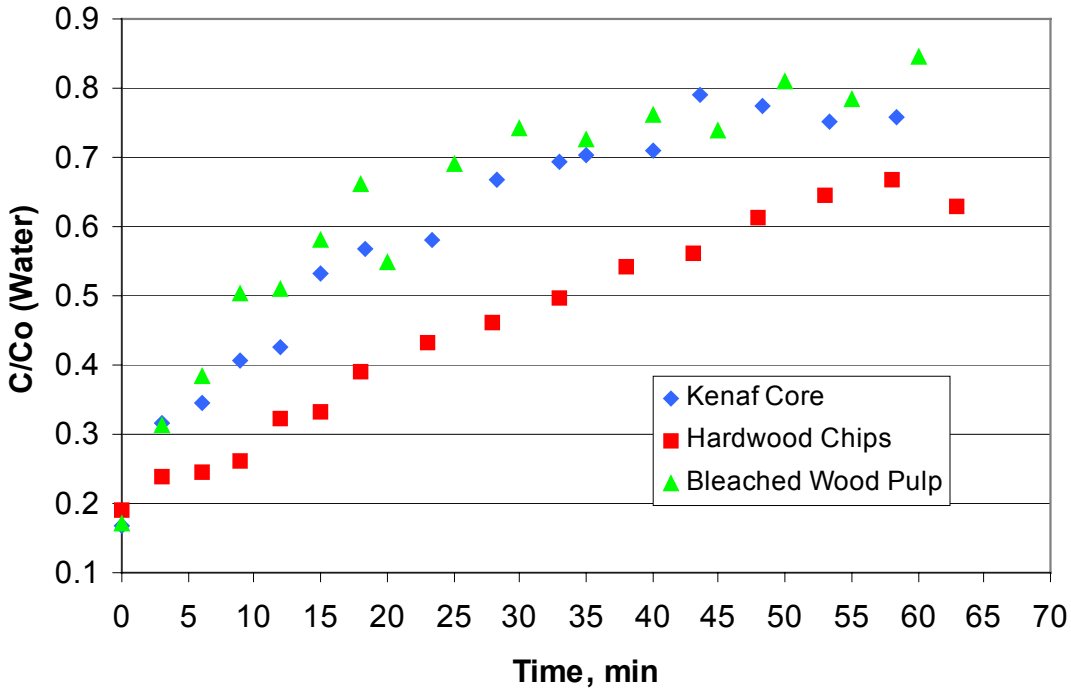

Figure 5.6. Breakthrough Curves Comparing the Capacities of the Adsorbents at an Initial Feed of 90 wt% Ethanol

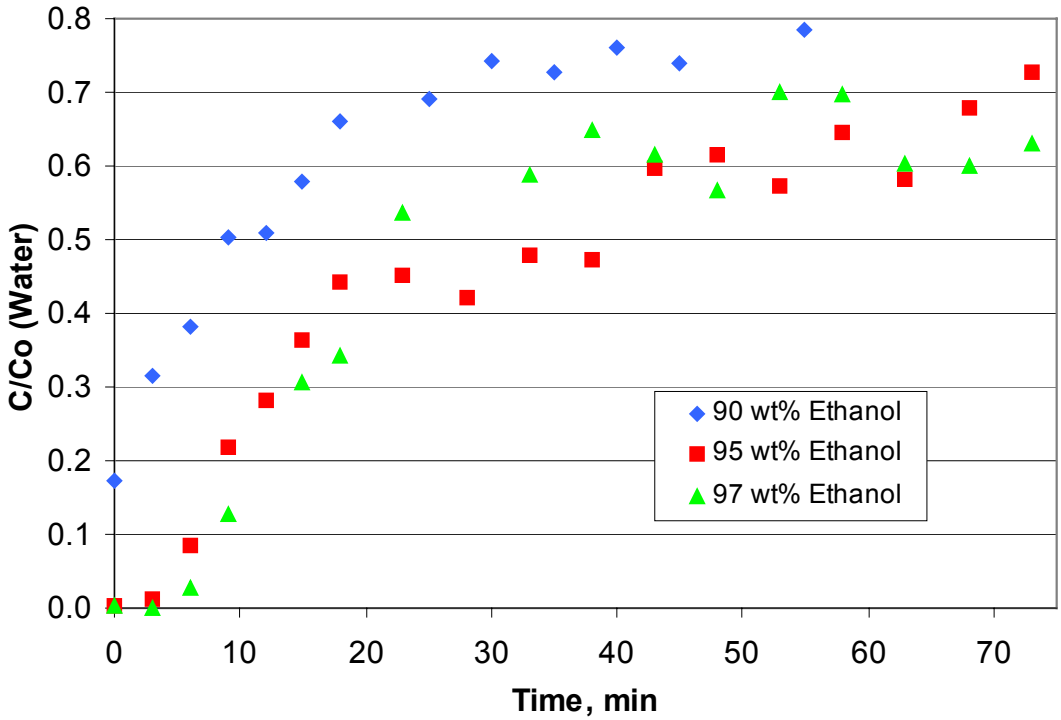

Figure 5.7. Breakthrough Curves Demonstrating Adsorption Characteristics Bleached Wood Pulp at Varying Concentrations of Ethanol

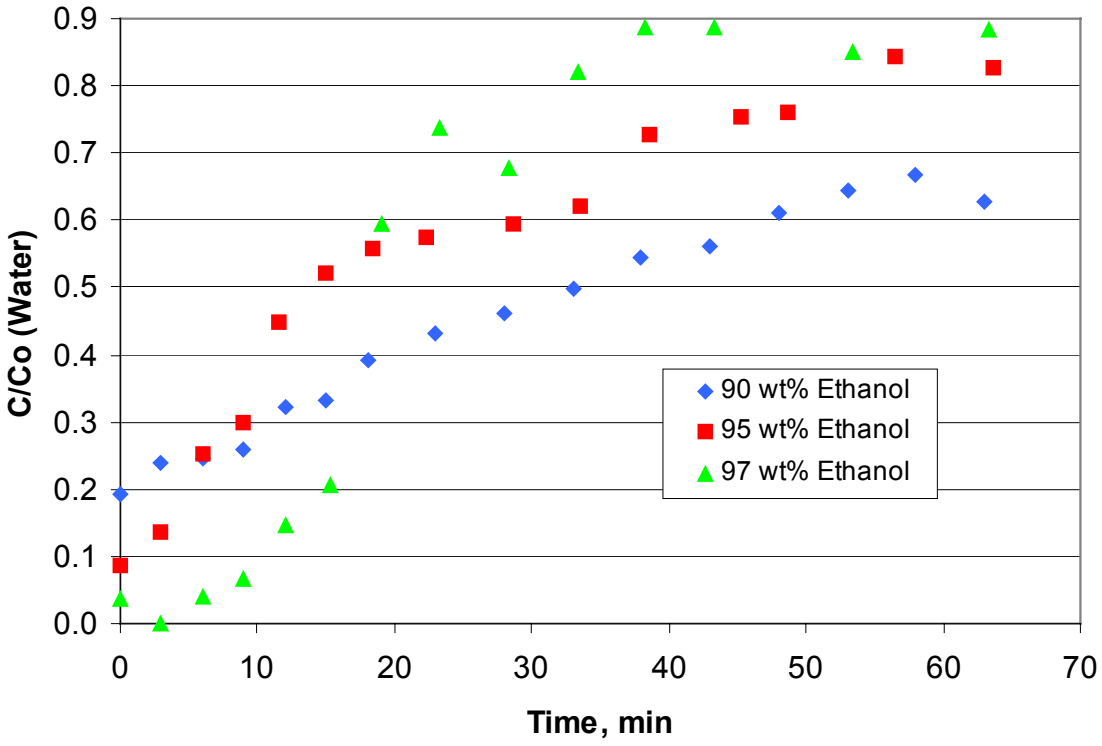

Figure 5.8. Breakthrough Curves Demonstrating Adsorption Characteristics for Hardwood Chips at Varying Concentrations of Ethanol

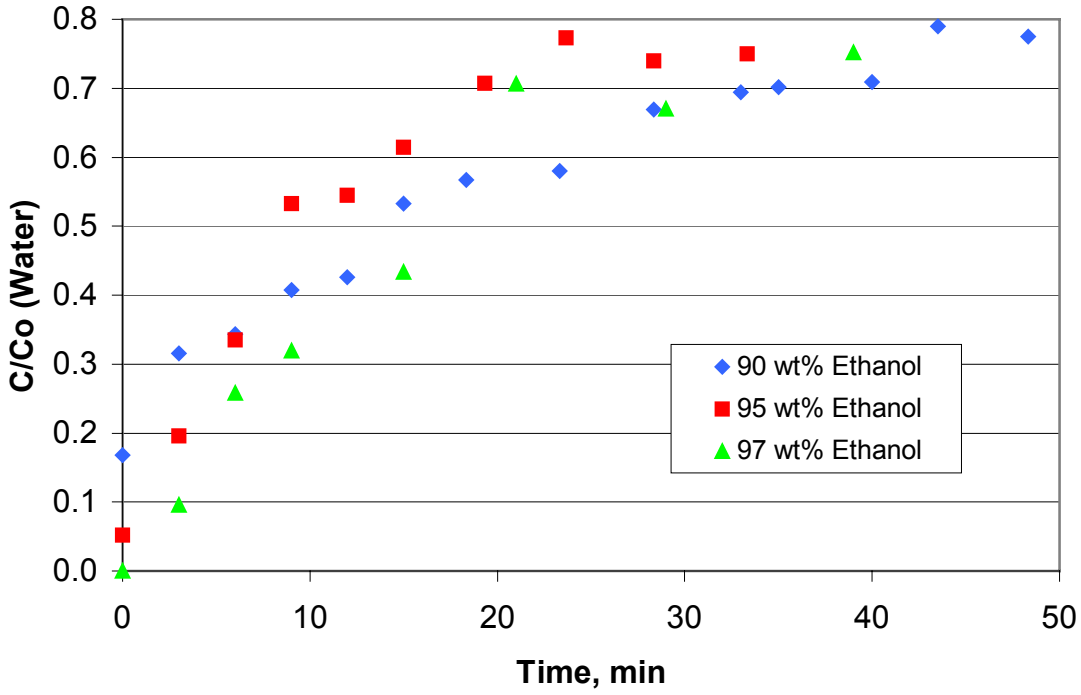

Figure 5.9. Breakthrough Curves Demonstrating Adsorption Characteristics for Kenaf Core at Varying Concentrations of Ethanol

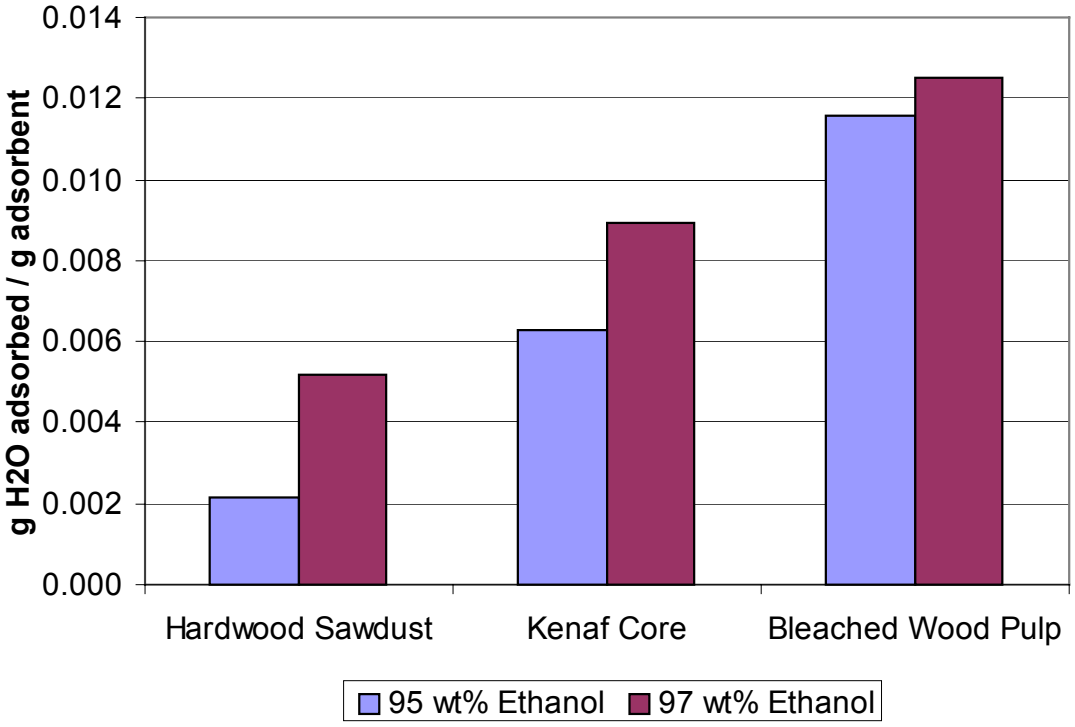

Figure 5.10. Water Loading at Breakthrough

Note: Breakthrough is defined as 99.5 wt% ethanol.

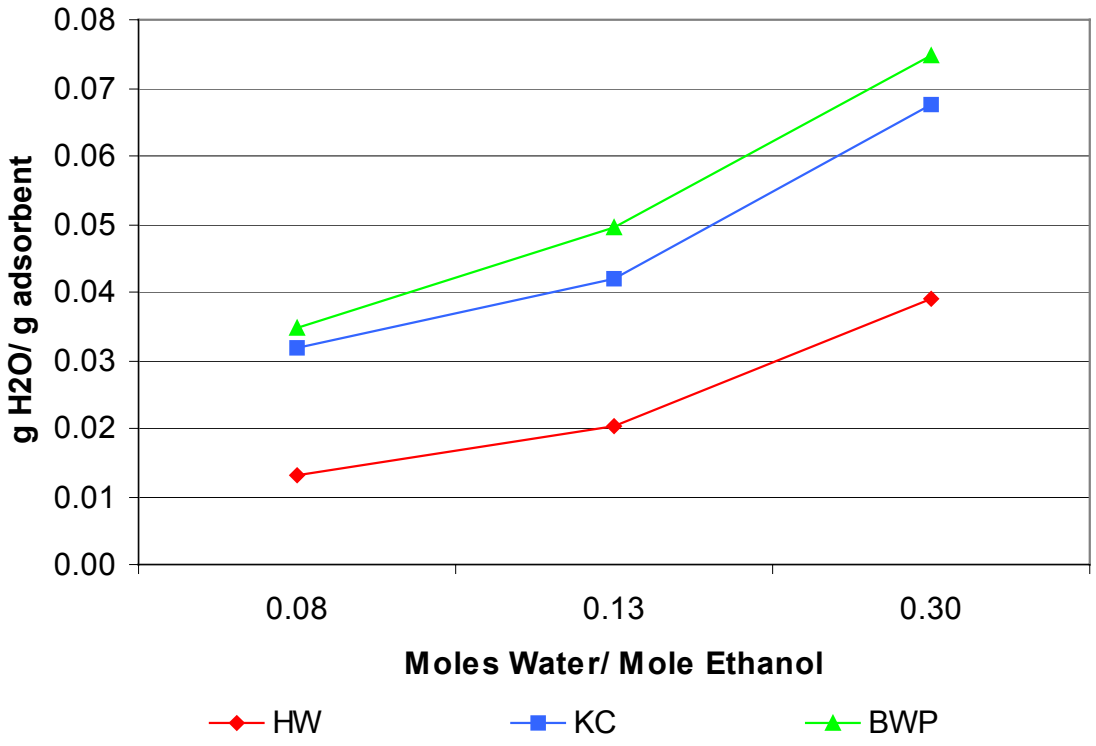

Figure 5.11. Vapor Phase Equilibrium Isotherms

Note: Equilibrium occurs at plateau of breakthrough curves.

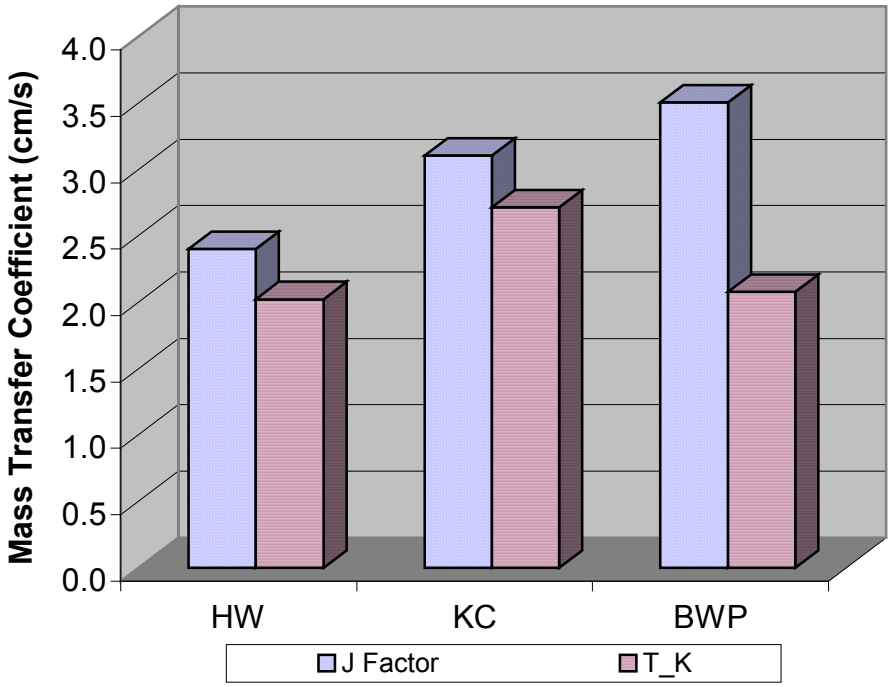

Figure 5.12. Comparison of the Mass Transfer Coefficient Determined from Two Different Correlations

Notes: 1. (J Factor) represents calculations based from the Colburn J Factor
2. (T_K) represents calculations based from the Thoenes-Kramers Correlation

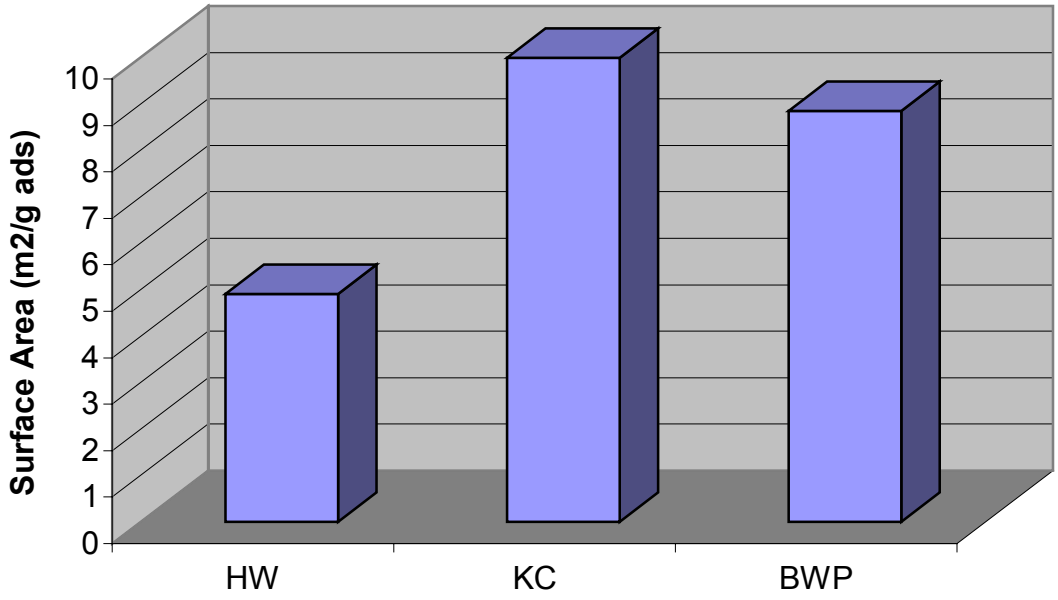

Figure 5.13. Surface Area of Adsorbents

CHAPTER VI

CONCLUSIONS

Conclusions

The following summarizes the significant results from this study that are important in explaining the adsorption of water from an ethanol/ water mixture after the distillation step.

1) Ligno-cellulosic materials possess an affinity towards water. Their hygroscopic nature allows for the uptake of water molecules from ethanol mixtures that are at least 10 percent, by weight, water.
2) All three materials studied, the hardwood sawdust, the kenaf core, and the bleached wood pulp, demonstrated the ability to preferentially adsorb water over ethanol. These materials all contain an abundance of hydroxyl groups from their molecular makeup that are necessary to adhere water molecules to the surface of the adsorbent.
3) At equilibrium, the bleached wood pulp adsorbs the most water, followed by the kenaf core and then the hardwood sawdust. There is not an appreciable difference between the bleached wood pulp and the kenaf core in the amount of water adsorbed; however, these two are significantly better than the hardwood sawdust at dehydrating ethanol.

4) At the threshold point, called breakthrough, the bleached wood pulp performed best, followed by the kenaf core and then the hardwood sawdust. This can only be stated for concentrations of 3 and 5 wt% water. There was insufficient data at the 10 wt% water due to equipment capability. The data did show adsorption of water at this concentration; however, it was an insufficient amount to produce ethanol with at least a 99.5 wt% purity. It is believed that an increase in column height, resulting in more adsorbent, would give similar results as the 95 and 97 wt% concentrations.
5) The length of the Mass Transfer Zone (MTZ) and the velocity at which it travels through the adsorbent bed increase with increasing concentrations of water. This is a rather intuitive observation. As the concentration of water increases, the adsorbent will reach its threshold at a much faster rate.
6) The bleached wood pulp has the shortest MTZ lengths and velocities, followed by the kenaf core and then the hardwood sawdust. All breakthrough curves are wide indicating long MTZ lengths. Longer adsorbent beds will make more efficient use of the bed capacity and lower regeneration costs.
7) On a per mass basis, the cellulosic adsorbents exceed the water adsorbing capacity of the starch-based adsorbents in the liquid phase equilibrium experiments.
8) In the vapor phase column experiments, only the bleached wood pulp demonstrated similar water adsorbing capacities. At breakthrough, the kenaf core and the hardwood sawdust adsorb on average 50% less water than the reported values for starch-based adsorbents.

9) Bleached wood pulp is a superior adsorbent over the kenaf core and hardwood sawdust in adsorbing water due to its large percentage of hydroxyl groups stemming from xylans and also because it has the largest external mass transfer coefficient.

In conclusion, cellulosic adsorbent materials offer an alternative approach for the dehydration of ethanol. In the presence of an adsorbent, water migrates from the ethanol/ water solution and adheres to the surface of the adsorbent particle. This, in turn, alters the thermodynamics of the ethanol/ water system and shifts the azeotropic point. Experimental evidence has shown that cellulosic biomass adsorbents possess a strong affinity towards water. The uptake of water is far greater than that of ethanol, and ethanol is, therefore, mostly unadsorbed.

Of the materials studied, the bleached wood pulp offers the most adsorbency; however, because of its swelling ability, care must be taken to keep the fluid in a vapor state to maintain adequate flow. Bleached wood pulp lacks the rigid structure that is associated with cellulosic materials containing lignin. Experimental observation has shown that cold spots within the adsorption column will condense the vapor, thus swelling the bleached wood pulp.

Engineering Significance of the Research

This study indicates the usefulness of using cellulosic biomaterials as adsorbents to remove water from ethanol in the 90 to 100 wt% ethanol region. Water showed to be adsorbed by bleached wood pulp, kenaf core, and hardwood sawdust. The uptake of water by the hardwood sawdust proved to be less favorable than the other two adsorbents.

The subject work has provided answers to the aforementioned questions. The dehydration of ethanol using cellulosic adsorbents establishes alternative adsorbents to starch-based adsorbents. The mechanism for water adsorption is essentially the same. The difference is that water molecules are attracted to hydroxyl groups found on xylans in cellulosic adsorbents and to hydroxyl groups found on amylopectin in starch adsorbents.

The calculation of the transport properties has led to the understanding of the adsorption phenomenon. The bleached wood pulp was found to have the shortest MTZ length, which will require the smallest bed volume in an adsorber.

In summary, this work is an indication that cellulosic materials are viable adsorbents for the removal of water in ethanol. While these experiments were conducted on the lab scale, limited information is obtainable. Pilot scale experiments are recommended to understand how the heat of adsorption will affect the adsorptive capacity and the rate of adsorption.

There may also be an economic incentive to use lingo-cellulosic adsorbents rather than starch adsorbents. Table 6.1 illustrates the costs of each of the adsorbents presented in this work. These prices are provided without the expense of transportation; therefore, depending on the location of the ethanol production facility, one adsorbent may be more economical than another.

Table 6.1. Adsorbent Prices

Adsorbent	Supplier	Bulk Cost ($/ lb)
Molecular Sieves	ECompressed Air	4.69
Kenaf Core	Kengro Corp.	0.92
Hardwood Sawdust[1]	-	0.46
Bleached Wood Pulp	Georgia Pacific	0.30
Starch Adsorbents[2]	-	0.10

Notes:
[1]The cost of hardwood sawdust has been estimated to be one-half of the cost of Kenaf core.
[2]The cost starch adsorbents have been estimated to be one-third the cost of bulk corn grits from Bunge Milling, Inc. in Danville, IL.

BIBLIOGRAPHY

Al-Rub, Fahmi A. Abu, Banat, Fawzi A., and Jumah, Rami, (1999), "Vapor-Liquid Equilibrium of ethanol-Water System in the Presence of Molecular Sieves," Separation Science and Technology, Vol. 34, pp. 2355 – 2368.

Banat, Fawzi A., Al-Rub, Fahmi A. Abu, and Simandl, Jana, (2000), "Analysis of Vapor-Liquid Equilibrium of Ethanol-water System via Headspace Gas Chromatography; Effect of Molecular Sieves," Separation and Purification Technology, Vol. 18, pp. 111 - 118.

Beery, Kyle E. and Ladisch, Michael R., (2001), "Adsorption of Water from Liquid – Phase Ethanol – Water Mixtures at Room Temperature Using Starch – Based Adsorbents," Industrial Engineering Chemical Research, Vol. 40, pp. 2112 – 2115.

Beery, Kyle E. and Ladisch, Michael R., (2001)"Chemistry and Properties of Starch Based Desiccants," Enzyme and Microbial technology, Vol. 28, pp. 573 – 581.

Berthold, J., Finaudo, M., Salmen, L., (1996), "Association of water to Polar Groups; Estimations By an Adsorption Model for Ligno-Cellulosic Materials," Colloids and Surfaces A: Physiochemical and Engineering Aspects, Vol. 112, pp. 117 – 129.

Bienkowski, P. R., Barthe, A., Voloch, M., Neuman, R. N. and Ladisch, M. R. (1986), "Breakthrough Behavior of 17.5 Mol%Water in Methanol, Ethanol, Isopropanol, and t-Butanol Vapors Passed Over Corn Grits," Biotechnology and Bioengineering, Vol. XXVIII, pp. 960 – 964.

Bird R. Byron, Stewart, Warren E., and Lightfoot, Edwin N., (1960), Transport Phenomenon, John Wiley and Sons, Inc.

Black, Cline, (1980), "Distillation Modeling of Ethanol Recovery and Dehydration Processes for Ethanol and gasohol," Chemical Engineering Progress.

Black, Cline and Ditsler, D. E., (1972), "Dehydration of Aqueous Ethanol Mixtures by Extractive Distillation," Advances in Chemistry, Ser. 115, pp 1 - 15.

Black, Cline, Golding, R.A., and Ditsler, D. E., (1972), "Azeotropic Distillation Results from Automatic Computer Calculations," Advances in Chemistry, Ser. 115, pp 64 – 92.

Carmo, M. J. and Gubulin, J. C., (1997), "Ethanol – Water Adsorption on Commercial 3A Zeolites: Kinetic and Thermodynamic Data," Brazilian Journal of Chemical Engineering, Vol. 14, No. 3.

Carmo, M. J. and Gubulin, J. C., (1997), "Kinetic and Thermodynamic Study on Adsorption by Starchy Materials in the ethanol – Water System," Brazilian Journal of Chemical Engineering, Vol. 14, No. 3.

Crawshaw, John P., and Hills, John H., (1989), "Sorption of Ethanol and Water by Starchy Materials," Industrial Engineering Chemical Research, Vol. 29, pp. 397 – 399.

Crittenden, Barry and Thomas, W. John, (1998), Adsorption Technology and Design, Butterworth Heinemann.

Crittenden, B. D. and Sowerby, B., (1990), "Scale-up of Vapor Phase Adsorption Columns for Breaking the Ethanol – Water Azeotrope," Institution of Chemical Engineers Symposium Series, N 118.

Czihak, C., Muller, M., Schober, H., Heux, L., Vogl, G., (1999), "Dynamics of Water Adsorbed to Cellulose," Physica B, Vol. 266, pp. 87 – 91.

Davis, Karl G. and Manchanda, Kristan D., (1974), "Unit Operation for Drying Fluids," Chemical Engineering, New York, McGraw Hill.

de Boer, J. H., (1953), The Dynamical Character of Adsorption, Oxford, Clarendon Press.

Dubinin, M. M., (1960), "The Potential Theory of Adsorption of Gases and Vapors for Adsorbents with Energetically Nonuniform Surfaces," Chemical Review, Vol. 60, pp. 235 - 241.

Fengel, Dietrich and Wegener, Gerd, (1984), Wood Chemistry, Ultrastructure, and Reactions, Berlin, Walter de Gruyter.

Fogler, H. Scott, (1999), Elements of Chemical Reaction Engineering, Prentice Hall PTR, Third Edition.

Freund, Rudolf J. and Wilson, William, J., (1997), Statistical Methods, Revised Edition,

Academic Press, San Diego.

Ferreira, Paulo J., Matos, Sandra, and Figueiredo, Margarida M., (1998), "Size Characterization of Fibers and Fines in Hardwood Kraft Pulps," Presented at the World Congress on Particle technology 3, Brighton, UK.

Garg, D. R. and Ausikaitis, J. P., (1983), "Molecular Sieve Dehydration Cycle for High Water Content Streams," Chemical Engineering Progress.

Gregg, S. J. and Sing, K. S., (1967), Adsorption, Surface Area, and Porosity, Academic Press, England.

Grethlein, Hans E. and Nelson, Thomas B., (1992), Projected Process Economics for Ethanol Production From Corn, Michigan Biotechnology Institute, USDA, Agricultural Research Service.

Han, James S., (1998), "Properties of Nonwood Fibers."

Han, James S. and Rowell, Jeffery S., (1996), "Chemical Composition of Fibers," Paper and Composites from Agro-Based Resources, Chapter 5, CRC Press.

http://www.eren.doe.gov/RE/bioenergy.html

Hong, J., Voloch, M., Ladisch, Michael R., and Tsao, G.T., (1982), "Adsorption of Ethanol-Water Mixtures by Biomass Materials," Biotechnology and Bioengineering, Vol. XXIV, pp. 725 - 730.

Hu, Xien and Weiguo, (2001), "Fixed-Bed Adsorption and Fluidized-Bed Regeneration for Breaking the Azeotrope of Ethanol and Water," Separation Science and Technology, Vol. 36, pp. 125 – 136.

Israelachvili, Jacob N., (1985), Intermolecular and Surface Forces: Applications to Colloidal and Biological Systems, Academic Press, London.

Kalutskaya, E. P., (1988), "Interaction Between Sorbed Water and Xylan Studied by IR Spectroscopy," Polymer Science U.S.S.R., Vol. 30, pp. 885 – 891.

Ladisch, Michael R., (1979), "Dehydration of Ethanol: New Approach Gives Positive Energy Balances," Science, Vol. 205, pp 898 – 900.

Ladisch, Michael R., Voloch, Marcio, Hong, Juan, Bienkowski, Paul, and Tsao, George T., (1984), "Cornmeal Adsorber for Dehydrating Ethanol Vapors," Industrial & Engineering Chemistry, Process Design and Development, Vol. 23, pp 437 – 443.

Ladisch, Michael R., and Tsao, G. T., (1982), U. S. Patent No. 4,345,973, "Vapor Phase

Dehydration of Aqueous Alcohol Mixtures," assigned to the Purdue Research Foundation.

Lee, Jay Y., Ladisch, Michael R., (1987), "Polysaccharides as Adsorbents: An Update on Fundamental Properties and Commercial Prospects," Biochemical Engineering V, Eds. M, L. Shuler and W. L. Weigand, The New York Academy of Sciences, pp. 492 - 498.

Lee, Jay Y., Westgate, Paul J., and Ladisch, Michael R., (1991), "Water and Ethanol Sorption Phenomena on Starch," AICHE Journal, Vol. 37, No. 8, pp 1187 – 1195.

Neuman, Robert, Voloch, Marcio, Bienkowski, Paul and Ladisch, Michael R., (1986), "Water Sorption Properties of a Polysaccharide Adsorbent," American Chemical Society.

Nikitin, N. I., (1966), The Chemistry of Cellulose and Wood, Israel.

Perry, Robert H., Green, Don W. and Maloney, James O., (1997), Perry's Chemical Engineer's Handbook, Seventh Edition, McGraw Hill, New York.

Rao, M. B., and Sircar, S., (1996), "Adsorption from Binary Immiscible Liquid Mixtures," AICHE Journal, Vol. 42, pp. 1191 - 1194.

Rao, M. B., and Sircar, S., (1992), "Production of Motor Fuel Grade Alcohol by Concentration Swing Adsorption," Separation Science and Technology, Vol. 27, pp. 1875 - 1887.

Rebar, V., Fischbach, E. R., Apostolopoulos, D., and Kikini, J. L., (1984), "Thermodynamics of Water and Ethanol Adsorption on Four Starches as Model Biomass Separation Systems," Biotechnology and Bioengineering, Vol. XXVI, pp. 513 – 517.

Reid, Robert C., Prausnitz, John M., Poling, Bruce E., (1987), Properties of Gases and Liquids, 2nd Edition, New York, McGraw-Hill.

Rowell, Roger M. and Han, James S., (1999), "Changes in Kenaf Properties and Chemistry as a Function of Growing Time," Kenaf Properties, Processing, and Products, Chapter 3, pp. 33 – 41.

Ruthven, Douglas M., (1984), Principles of Adsorption and Adsorption Processes, New York, Wiley.

Schweitzer, Philip A., (1996), Handbook of Separation Techniques for Chemical Engineers, Third Edition, New York McGraw Hill.

Smith, Edward H., (1996), "Wave Front Analysis for Design of Fixed-Bed Adsorbers," Chemical Engineering Communications, Vol. 159, pp. 17 - 37.

Veluraja, K., and Atkins, E. D. T., (1987), "Helical Structure of (1 - 3) Xylan and the Water Mediated Hydrogen Bonding Schemes," Carbohydrate Polymers, Vol. 7, pp. 133 - 141.

van Winkle, Mathew, (1967), Distillation, New York McGraw Hill.

Vareli, G., Demertizis, P. G., and Akrida-Demertzi, K., (2000), "Effect of Regeneration Thermal Treatment of Cellulosic and Starchy Materials on their Capacity to Separate Water and Ethanol," Journal of Cereal Science, Vol. 31, pp. 147 – 154.

Wankat, Phillip C., (1998), Separations in Chemical Engineering: Equilibrium Staged Processes, Prentice Hall, Inc.

Westgate. P., Lee J. Y., and Ladisch, M. R., (1992), "Modeling of Equilibrium Sorption of Water Vapor on Starch Materials," Transactions of the American Society of Agricultural Engineers, Vol. 35, pp. 213 - 218.

APPENDIX A

SCANNING ELECTRON MICROGRAPHS OF ADSORBENTS

Figure A.1. S.E.M. of Hardwood Sawdust at 150X Magnification

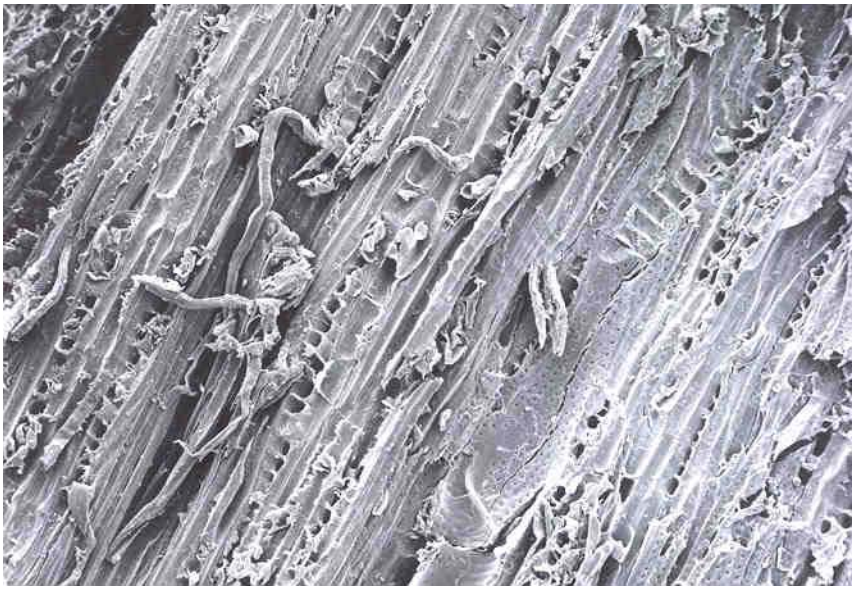

Figure A.2. S.E.M. of Bleached Wood Pulp at 150X Magnification

Figure A.3. S.E.M. of Bleached Wood Pulp at 800X Magnification

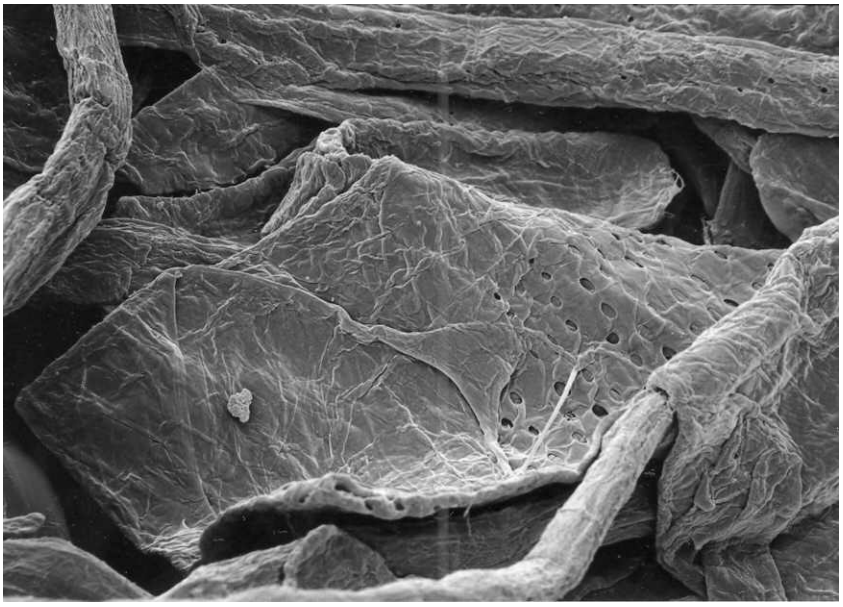

Figure A.4. S.E.M. of Kenaf Core at 100X Magnification

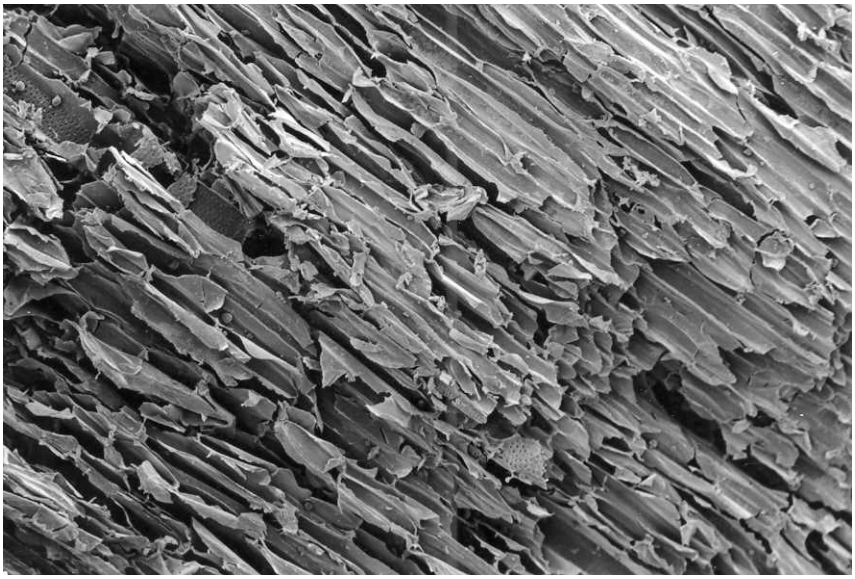

Figure A.5. S.E.M. of Kenaf Core at 150X Magnification

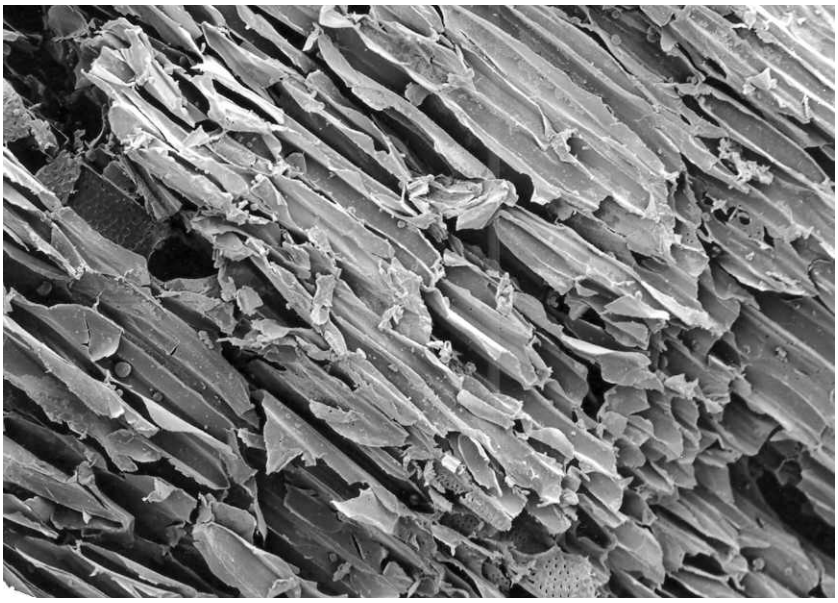

APPENDIX B

SUMMARY OF EXPERIMENTAL DATA FOR BATCH LIQUID PHASE EXPERIMENTS

Table B.1. Experimental Data for Batch Liquid Phase Experiments Using Molecular Sieves

Mixture Density (g / cm3)	Mass of Liquid (g)	Mass of Adsorbent (g)	Initial Ethanol Concentration (mass fraction)	Final Ethanol Concentration (mass fraction)
0.791	1.581	2.00	0.996	1.002
0.791	1.581	2.00	0.996	1.001
0.791	1.581	2.00	0.996	0.998
0.793	1.586	2.00	0.975	1.010
0.793	1.586	2.00	0.975	1.006
0.793	1.586	2.00	0.975	1.000
0.797	1.593	2.00	0.952	0.995
0.797	1.593	2.00	0.952	0.995
0.797	1.593	2.00	0.952	1.007
0.806	1.612	2.00	0.879	0.948
0.806	1.612	2.00	0.879	0.955
0.806	1.612	2.00	0.879	0.934
0.824	1.648	2.00	0.795	0.863
0.824	1.648	2.00	0.795	0.866
0.824	1.648	2.00	0.795	0.868
0.842	1.685	2.00	0.682	0.743
0.842	1.685	2.00	0.682	0.763
0.842	1.685	2.00	0.682	0.750

Table B.2. Experimental Data for Batch Liquid Phase Experiments Using Kenaf Core

Mixture Density	Mass of Liquid	Mass of Adsorbent	Initial Ethanol Concentration	Final Ethanol Concentration
(g / cm3)	(g)	(g)	(mass fraction)	(mass fraction)
0.791	3.953	0.50	0.990	0.992
0.791	3.953	0.50	0.990	0.993
0.791	3.953	0.50	0.990	0.990
0.793	3.966	0.50	0.970	0.982
0.793	3.966	0.50	0.970	0.982
0.793	3.966	0.50	0.970	0.977
0.797	3.983	0.50	0.954	0.967
0.797	3.983	0.50	0.954	0.963
0.797	3.983	0.50	0.954	0.969
0.806	4.030	0.50	0.913	0.926
0.806	4.030	0.50	0.913	0.934
0.806	4.030	0.50	0.913	0.931
0.824	4.119	0.50	0.822	0.838
0.824	4.119	0.50	0.822	0.841
0.824	4.119	0.50	0.822	0.840
0.842	4.212	0.50	0.750	0.762
0.842	4.212	0.50	0.750	0.766
0.842	4.212	0.50	0.750	0.765

Table B.3. Experimental Data for Batch Liquid Phase Experiments Using Hardwood Sawdust

Mixture Density (g / cm3)	Mass of Liquid (g)	Mass of Adsorbent (g)	Initial Ethanol Concentration (mass fraction)	Final Ethanol Concentration (mass fraction)
0.791	3.163	0.50	0.988	0.992
0.791	3.163	0.50	0.988	0.986
0.791	3.163	0.50	0.988	0.992
0.793	3.173	0.50	0.983	0.991
0.793	3.173	0.50	0.983	0.982
0.793	3.173	0.50	0.983	0.979
0.797	3.186	0.50	0.965	0.970
0.797	3.186	0.50	0.965	0.970
0.797	3.186	0.50	0.965	0.975
0.806	3.224	0.50	0.876	0.885
0.806	3.224	0.50	0.876	0.886
0.806	3.224	0.50	0.876	0.886
0.824	3.295	0.50	0.797	0.813
0.824	3.295	0.50	0.797	0.805
0.824	3.295	0.50	0.797	0.811
0.842	3.369	0.50	0.688	0.700
0.842	3.369	0.50	0.688	0.693
0.842	3.369	0.50	0.688	0.698

Table B.4. Experimental Data for Batch Liquid Phase Experiments Using Bleached Wood Pulp

Mixture Density (g / cm3)	Mass of Liquid (g)	Mass of Adsorbent (g)	Initial Ethanol Concentration (mass fraction)	Final Ethanol Concentration (mass fraction)
0.791	3.953	0.40	0.991	0.989
0.791	3.953	0.40	0.991	0.992
0.791	3.953	0.40	0.991	0.994
0.793	3.966	0.40	0.968	0.976
0.793	3.966	0.40	0.968	0.977
0.793	3.966	0.40	0.968	0.981
0.797	3.983	0.40	0.947	0.954
0.797	3.983	0.40	0.947	0.967
0.797	3.983	0.40	0.947	0.964
0.806	4.030	0.40	0.860	0.889
0.806	4.030	0.40	0.860	0.883
0.806	4.030	0.40	0.860	0.885
0.824	4.119	0.40	0.782	0.807
0.824	4.119	0.40	0.782	0.798
0.824	4.119	0.40	0.782	0.803
0.842	4.212	0.40	0.669	0.692
0.842	4.212	0.40	0.669	0.692
0.842	4.212	0.40	0.669	0.689

APPENDIX C

SUMMARY OF EXPERIMENTAL DATA FOR BATCH VAPOR PHASE ADSORPTION COLUMN EXPERIMENTS

Table C.1. Experimental Data for Batch Vapor Phase Column Experiments Using Kenaf Core

Time (min)	C/C_o (Concentration of Water)		
	$C_o = 0.03$	$C_o = 0.05$	$C_o = 0.10$
0	0.000	0.052	0.168
3	0.096	0.196	0.316
6	0.258	0.335	0.344
9	0.319	0.533	0.407
12	-	0.545	0.426
15	0.434	0.614	0.533
19	0.443	0.707	0.567
24	0.670	0.773	0.580
29	0.752	0.739	0.669
34	-	0.750	0.694
39	0.752	0.812	0.709
44	0.834	-	0.790
49	-	0.836	0.775
54	0.885	0.819	0.752
59	0.914	0.867	0.760
64	0.815	0.817	-

Table C.2. Experimental Data for Batch Vapor Phase Column Experiments Using Hardwood Sawdust

Time (min)	C/C_o (Concentration of Water)		
	$C_o = 0.03$	$C_o = 0.05$	$C_o = 0.10$
0	0.035	0.087	0.191
3	0.001	0.136	0.240
6	0.039	0.253	0.244
9	0.067	0.300	0.260
12	0.146	0.447	0.323
15	0.206	0.522	0.332
19	0.593	0.559	0.391
24	0.736	0.574	0.432
29	0.677	0.594	0.460
34	0.820	0.621	0.498
39	0.886	0.727	0.544
44	0.887	0.752	0.560
49	-	0.762	0.612
54	0.849	-	0.644
59	0.941	0.843	0.668
64	0.884	0.828	0.629

Table C.3. Experimental Data for Batch Vapor Phase Column Experiments Using Bleached Wood Pulp

Time (min)	C/C_o (Concentration of Water)		
	$C_o = 0.03$	$C_o = 0.05$	$C_o = 0.10$
0	0.003	0.002	0.172
3	0.000	0.012	0.314
6	0.028	0.085	0.383
9	0.126	0.218	0.503
12	-	0.281	0.509
15	0.306	0.365	0.579
19	0.342	0.443	0.661
24	0.538	0.451	0.689
29	-	0.423	0.742
34	0.589	0.480	0.727
39	0.649	0.473	0.762
44	0.614	0.595	0.738
49	0.567	0.614	0.808
54	0.700	0.572	0.785
59	0.698	0.645	0.844
64	0.602	0.582	-

APPENDIX D

GAS CHROMATOGRAPH CALIBRATION AND OPERATING CONDITIONS

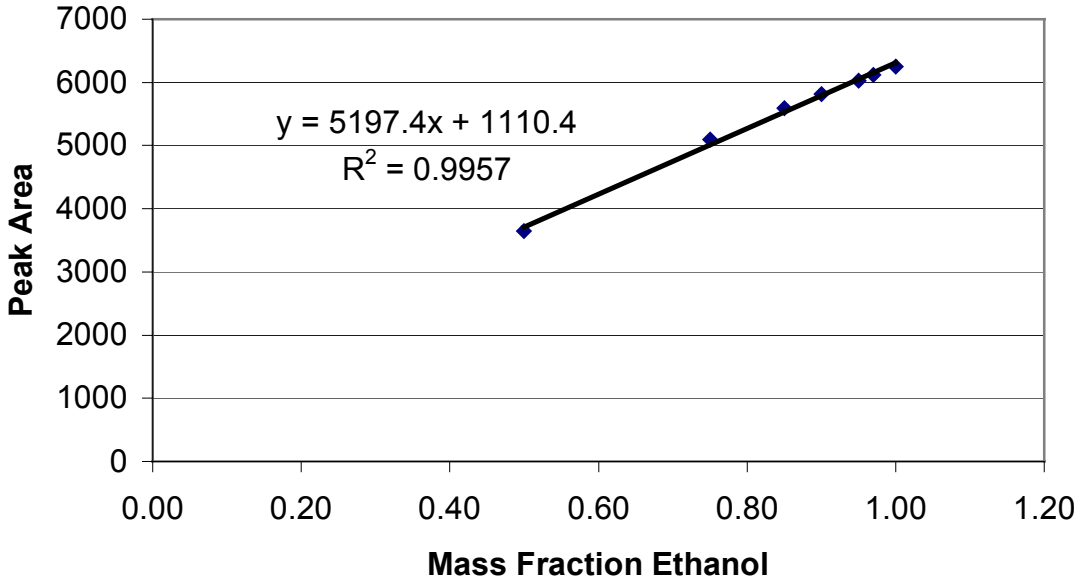

Figure D.1. Gas Chromatograph Calibration Curve for Measuring Concentrations of Ethanol

The operating conditions that have been set on the Gas Chromatograph (GC) for the analysis of ethanol containing water are given below.

HP 6890 Series: HP – Innowax Capillary Column, Flame Ionization Detector

For detection of ethanol:

Initial Column Temperature:	45°C
Initial Column Holding Time:	2.00 min
Column Temperature Programming:	20°C/ min
Final Column Temperature:	110°C
Final Column Holding Time:	2.00 min
Injection Temperature:	250°C
Detector Temperature:	250°C
Sample Volume Injected:	0.50 micro liter
Split Ratio:	100: 1
Flow Rates	
Column Flow:	31 ml/ min
Split Flow:	132.0 ml/ min
Helium (Carrier Gas) Flow:	45.0 ml/ min
Hydrogen Flow:	40.0 ml/ min
Air Flow:	450.0 ml/ min

APPENDIX E

SUPPLEMENTARY RESULTS AND INFORMATION

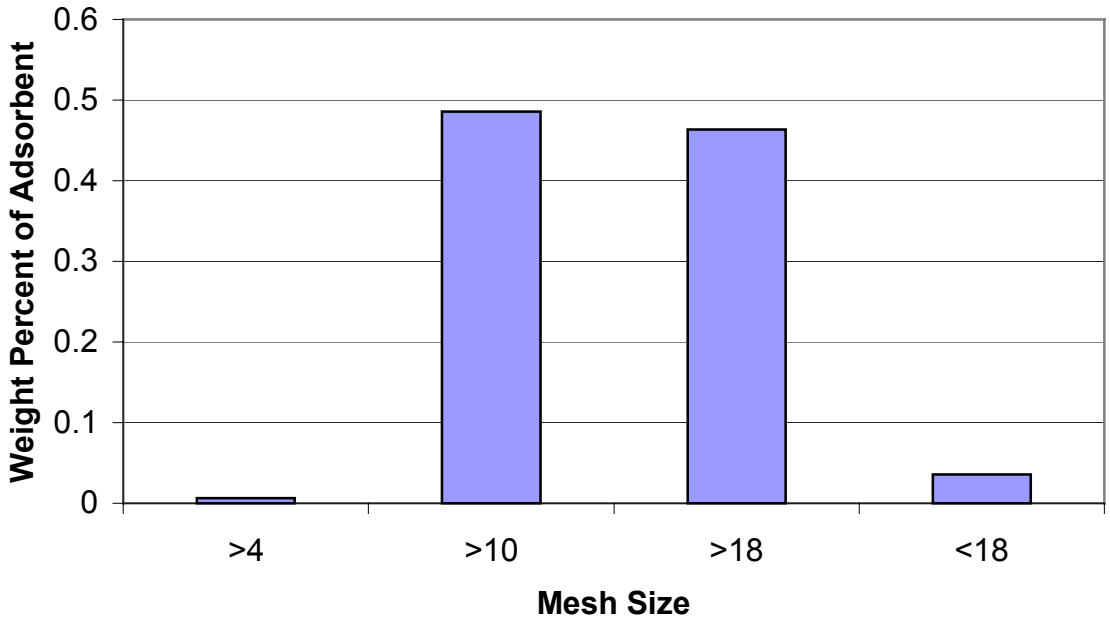

Figure E.1. Particle Size Distribution for Hardwood Sawdust

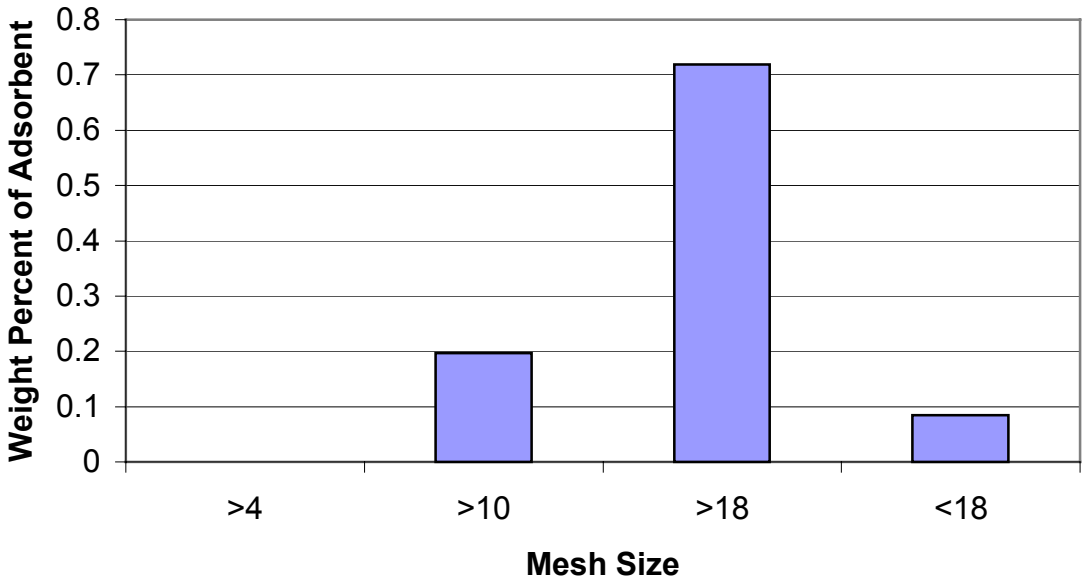

Figure E.2. Particle Size Distribution for Kenaf Core

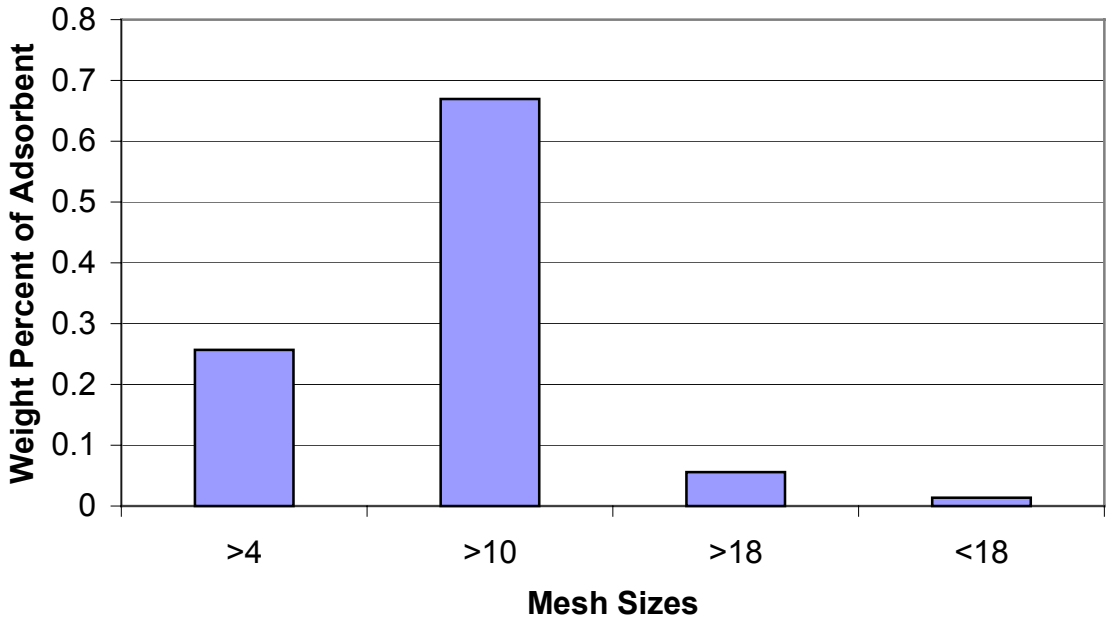

Figure E.3. Particle Size Distribution for Bleached Wood Pulp

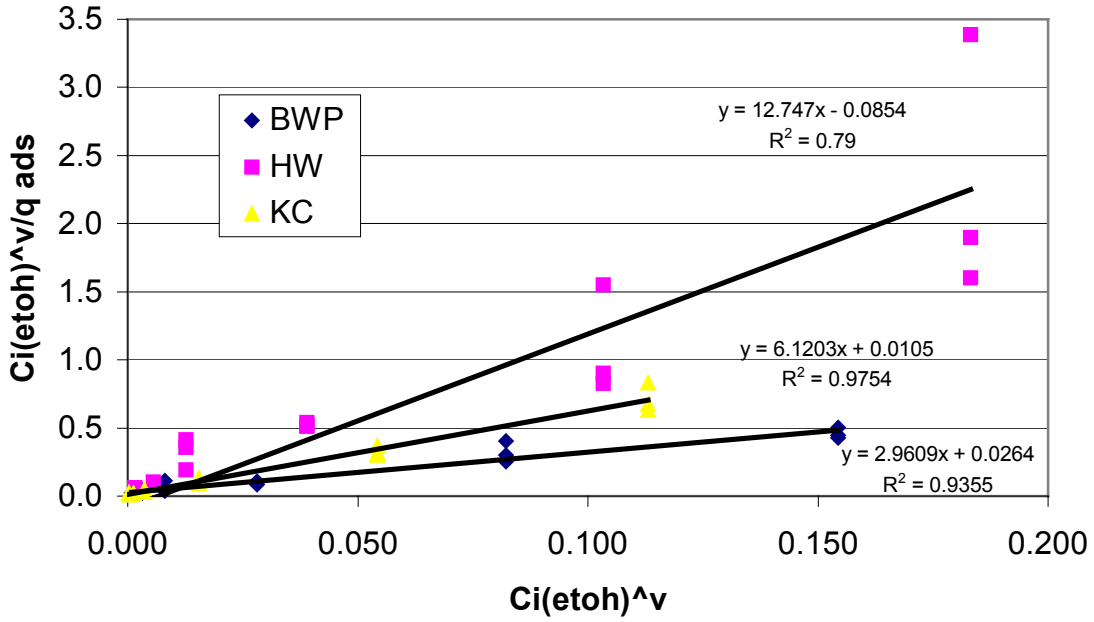

Figure E.4. Linearized Chakravarti – Dhar Isotherms for Liquid Phase Experiments

Notes:

- C_i (etoh)^v is the mass fraction of ethanol raised to a power known as a Chakravarti – Dhar isotherm parameter. This parameter is calculated by regression.
- q ads is the mass of water adsorbed per mass of adsorbent

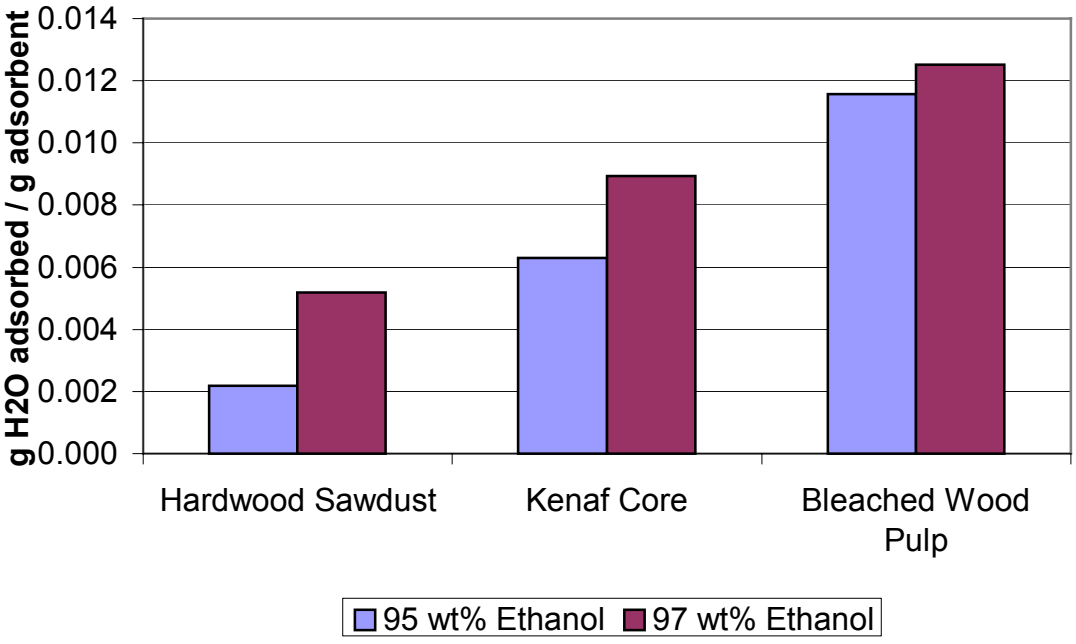

Figure E.5. Water Loading at Breakthrough

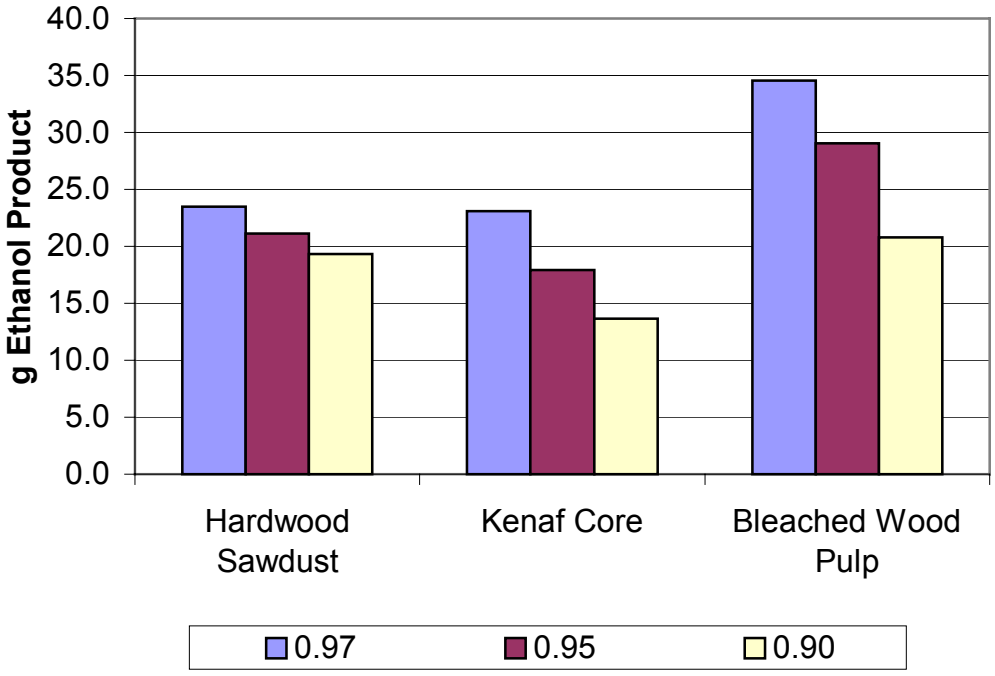

Figure E.6. Mass of Ethanol, in grams, Obtained from Vapor Phase Column Experiments at Equilibrium

Table E.1. Mass Transport Parameters Used in Determining the Mass Transfer of Water Vapor through the Porous Matrix of the Adsorbents

Adsorbent	Mass Fraction Ethanol	Mixture Viscosity (Poise)	Mean Particle Diameter (cm)	Mass Velocity (g/ cm^2 s)
Hardwood	0.97	1.073E-04	0.219	1.70E-03
Hardwood	0.95	1.075E-04	0.219	2.06E-03
Hardwood	0.90	1.081E-04	0.219	1.99E-03
Kenaf Core	0.97	1.073E-04	0.162	2.47E-03
Kenaf Core	0.95	1.075E-04	0.162	2.44E-03
Kenaf Core	0.90	1.081E-04	0.162	2.62E-03
Bleached Wood Pulp	0.97	1.073E-04	0.223	2.57E-03
Bleached Wood Pulp	0.95	1.075E-04	0.223	2.64E-03
Bleached Wood Pulp	0.90	1.081E-04	0.223	2.22E-03

Table E.2. Mass Transfer Characteristics (Dimensionless Parameters and External Mass Transfer Coefficient, K_c)

Adsorbent	Mass Fraction Ethanol	Reynolds Number	Schmidt Number	Sherwood Number	Colburn J Factor	K_c[1] (cm/s)	K_c[2] (cm/s)
Hardwood	0.97	3.463	0.443	2.851	1.098	2.021	1.988
Hardwood	0.95	4.194	0.444	2.937	1.196	2.669	2.049
Hardwood	0.90	4.021	0.446	2.919	1.174	2.515	2.036
Kenaf Core	0.97	3.741	0.443	2.885	1.137	3.044	2.710
Kenaf Core	0.95	3.690	0.444	2.879	1.130	2.986	2.705
Kenaf Core	0.90	3.936	0.446	2.910	1.163	3.285	2.733
Bleached Wood Pulp	0.97	5.320	0.443	3.055	1.330	3.697	2.094
Bleached Wood Pulp	0.95	5.469	0.444	3.070	1.346	3.851	2.105
Bleached Wood Pulp	0.90	4.566	0.446	2.980	1.243	2.972	2.043

Notes: [1] These values for the external mass transfer coefficient were determined from the Colburn J Factor correlation.

[2] These values for the external mass transfer coefficient were determined from the Thoenes – Kramer correlation.